

Loss of stromal caveolin-1 leads to oxidative stress, mimics hypoxia and drives inflammation in the tumor microenvironment, conferring the “reverse Warburg effect”

A transcriptional informatics analysis with validation

Stephanos Pavlides,^{1,2} Aristotelis Tsirigos,³ Iset Vera,⁴ Neal Flomenberg,⁵ Philippe G. Frank,^{1,2} Mathew C. Casimiro,^{1,2} Chenguang Wang,^{1,2} Paolo Fortina,^{1,2} Sankar Addya,^{1,2} Richard G. Pestell,^{1,2} Ubaldo E. Martinez-Outschoorn,⁵ Federica Sotgia^{1,2,*} and Michael P. Lisanti^{1,2,5,6,*}

¹Departments of Stem Cell Biology and Regenerative Medicine; and Cancer Biology; ²The Jefferson Stem Cell Biology and Regenerative Medicine Center; and ⁵Department of Medical Oncology; Kimmel Cancer Center; Thomas Jefferson University; Philadelphia, PA USA; ³Computational Genomics Group; IBM Thomas J. Watson Research Center; Yorktown Heights, NY USA; ⁴Department of Microbiology and Immunology; Albert Einstein College of Medicine; New York, NY USA; ⁶Manchester Breast Centre and Breakthrough Breast Cancer Research Unit; Paterson Institute for Cancer Research; School of Cancer; Enabling Sciences and Technology; Manchester Academic Health Science Centre; University of Manchester, UK

Key words: caveolin-1, tumor stroma, myofibroblast, cancer associated fibroblast, oxidative stress, hypoxia, inflammation, mitochondrial dysfunction, Alzheimer disease, fibrosis, scleroderma, systemic sclerosis

Cav-1 (-/-) deficient stromal cells are a new genetic model for myofibroblasts and cancer-associated fibroblasts. Using an unbiased informatics analysis of the transcriptional profile of Cav-1 (-/-) deficient mesenchymal stromal cells, we have now identified many of the major signaling pathways that are activated by a loss of Cav-1, under conditions of metabolic restriction (with low glucose media). Our informatics analysis suggests that a loss of Cav-1 induces oxidative stress, which mimics a constitutive pseudo-hypoxic state, leading to (1) aerobic glycolysis and (2) inflammation in the tumor stromal microenvironment. This occurs via the activation of two major transcription factors, namely HIF (aerobic glycolysis) and NF κ B (inflammation) in Cav-1 (-/-) stromal fibroblastic cells. Experimentally, we show that Cav-1 deficient stromal cells may possess defective mitochondria, due to the over-production of nitric oxide (NO), resulting in the tyrosine nitration of the mitochondrial respiratory chain components (such as complex I). Elevated levels of nitro-tyrosine were observed both in Cav-1 (-/-) stromal cells, and via acute knock-down with siRNA targeting Cav-1. Finally, metabolic restriction with mitochondrial (complex I) and glycolysis inhibitors was synthetically lethal with a Cav-1 (-/-) deficiency in mice. As such, Cav-1 deficient mice show a dramatically reduced mitochondrial reserve capacity. Thus, a mitochondrial defect in Cav-1 deficient stromal cells could drive oxidative stress, leading to aerobic glycolysis, and inflammation, in the tumor microenvironment. These stromal alterations may underlie the molecular basis of the “reverse Warburg effect”, and could provide the key to targeted anti-cancer therapies using metabolic inhibitors. In direct support of these findings, the transcriptional profile of Cav-1 (-/-) stromal cells overlaps significantly with Alzheimer disease, which is characterized by oxidative stress, NO over-production (peroxynitrite formation), inflammation, hypoxia and mitochondrial dysfunction. We conclude that Cav-1 (-/-) deficient mice are a new whole-body animal model for an activated lethal tumor microenvironment, i.e., “tumor stroma” without the tumor. Since Cav-1 (-/-) mice are also an established animal model for profibrotic disease, our current results may have implications for understanding the pathogenesis of scleroderma (systemic sclerosis) and pulmonary fibrosis, which are also related to abnormal mesenchymal stem cell function.

Introduction

It is now well-recognized that the tumor micro-environment plays a critical role in tumor initiation, progression, and even metastasis, in many types of human cancers.¹⁻³ However, the tumor micro-environment is complex and heterogeneous,

consisting of numerous distinct cell types, including fibroblasts, endothelia, smooth muscle cells, as well as different immune/inflammatory cell types, such as macrophages.⁴ In this plethora of diversity, the myofibroblast or cancer-associated fibroblast has taken “center stage” as a determinant of outcome in human breast cancers.

*Correspondence to: Federica Sotgia and Michael P. Lisanti; Email: federica.sotgia@jefferson.edu and michael.lisanti@kimmelcancercenter.org

Submitted: 03/18/10; Accepted: 03/22/10

Previously published online: www.landesbioscience.com/journals/cc/article/2540

Recently, we identified a loss of caveolin-1 (Cav-1) as a molecular marker for the cancer-associated fibroblast phenotype.⁵ In this study, cancer-associated fibroblasts isolated from 8 out of 11 breast cancer patients showed a consistent and significant down-regulation of Cav-1, at the protein product level, but not at the transcriptional level.⁵ Similarly, Cav-1 deficient mammary fibroblasts generated from Cav-1 (-/-) null mice shared numerous properties with human breast cancer-associated fibroblasts, including hyper-proliferation, as well as a constitutive myofibroblastic phenotype, characterized by increased collagen production and activated TGFbeta signaling.⁶ Conditioned media prepared from Cav-1 (-/-) mammary fibroblasts was rich in pro-proliferative, pro-angiogenic, and pro-inflammatory growth factors and functionally promoted an EMT (epithelial-mesenchymal transition) in genetically normal primary cultures of mammary epithelial cells.⁶ Thus, Cav-1 (-/-) deficient mammary fibroblasts behave as cancer-associated fibroblasts and can alter the phenotype of adjacent epithelial cells by paracrine signaling events.⁶

To better understand the potential clinical significance of these findings, we assessed the prognostic value of a loss of Cav-1 expression in the cancer-associated fibroblast compartment in a well-annotated cohort of human breast cancer patients, with nearly 20 years of follow-up data.⁷ Surprisingly, our results showed that a loss of stromal Cav-1 was a powerful single independent predictor of early tumor recurrence, lymph node metastasis, tamoxifen-resistance, and poor clinical outcome, in human breast cancer patients.⁷ Importantly, these findings were independent of epithelial marker status, demonstrating that a loss of stromal Cav-1 has significant prognostic value in all the different sub-types of human breast cancer, including ER (+), HER2 (+) and triple-negative patients.⁷ A loss of stromal Cav-1 was a particularly powerful predictor in lymph-node positive patients, where an ~11.5-fold stratification of 5-year progression free survival was observed (80% survival for stromal Cav-1 (+) versus 7% survival for stromal Cav-1 (-)).⁷ Thus, a loss of stromal Cav-1 is a powerful predictor of tumor progression and metastasis.⁸

To determine if a loss of stromal Cav-1 also plays a critical role in tumor initiation, we also evaluated its clinical value in a DCIS patient cohort that was treated only with wide-excision, but without any radiation or chemotherapy.⁹ Remarkably, in this patient cohort, a loss of stromal Cav-1 was associated with a recurrence rate of 100%, and a progression rate (to invasive breast cancer) of 80%. As such, a loss of stromal Cav-1 could be used to predict DCIS progression to invasive breast cancer nearly 15–20 years in advance.⁹ Conversely, high stromal Cav-1 levels appeared to be protective against recurrence and progression. Thus, the use of stromal Cav-1 levels as a diagnostic and prognostic indicator, may also have implication for DCIS and breast cancer patient treatment stratification.⁹ Similar results were also obtained in human prostate cancer patients, where a loss of stromal Cav-1 was associated with advanced prostate cancer, as well as local and distant cancer cell metastasis.¹⁰ Thus, a loss of stromal Cav-1 may be a “barometer” for a highly-aggressive lethal tumor micro-environment phenotype that may be common to many different types of human cancer.⁸

As such, it will be important to understand mechanistically exactly how a loss of stromal Cav-1 could initiate these events, such as tumor progression and metastasis. Thus, we turned again to Cav-1 (-/-) deficient mice as a model system. As cancer-associated fibroblasts are thought to derive or evolve from mesenchymal stem cells, we isolated bone marrow derived stromal cells from matched Cav-1 (+/+) and Cav-1 (-/-) mice.¹¹ As mesenchymal stem cells prefer low-glucose media, they were cultured in alpha-MEM which has a low concentration of glucose (~5.5 mM). These wild-type and Cav-1 deficient stromal cells were then subjected to unbiased proteomic analysis that was also validated independently by genome-wide transcriptional profiling.¹¹ We speculated that this approach could provide insight into how a loss of Cav-1 in stromal cells could affect paracrine signaling, without the need for co-culture studies.

Proteomic analysis validated the idea that a loss of stromal Cav-1 confers a constitutive myofibroblast phenotype, as 8 known myofibroblast markers were upregulated (vimentin, calponin2, tropomyosin2/beta, gelsolin, prolyl 4-hydroxylase (P4ha1), collagen I (Col1a1 and Col1a2), and SPARC).¹¹ In addition, proteomic analysis also revealed the concomitant upregulation of 8 glycolytic enzymes associated with pyruvate and lactate production (aerobic glycolysis; a.k.a., the Warburg effect), including lactate dehydrogenase (Ldha) and the M2-isoform of pyruvate kinase (PkM2).¹¹ Finally, two markers of oxidative stress were increased, namely catalase and peroxiredoxin1.¹¹ Interestingly, there was a strong correspondence between our results from proteomics and transcriptional profiling, providing an indication that certain key transcription factors may be involved.¹¹ Transcriptional profiling also validated the expression of numerous cancer-associated fibroblast and inflammatory markers, such as Cxcl9, Ccl5 and Cxcl12 (SDF-1), among others.¹¹

Based on these findings, we proposed a new model to understand the Warburg effect in cancer biology, which we have now termed the “reverse Warburg effect”.¹¹ In this scenario, cancer-associated fibroblasts undergo aerobic glycolysis to produce energy-rich metabolites that can then be transferred, via secretion, to the TCA cycle of cancer cells (undergoing oxidative phosphorylation).¹¹ This new idea could explain how a loss of stromal Cav-1 leads to poor clinical outcome, as the tumor stroma would literally “feed” the cancer cells.¹¹

Here, we have re-interrogated the transcriptional profiling¹¹ of matched wild-type and Cav-1 (-/-) deficient bone marrow-derived stromal cells to unravel which transcriptional programs are activated by a loss of stromal Cav-1, using an informatics approach. Based on this informatics analysis, we now propose that a loss of stromal Cav-1 leads to oxidative stress which can then activate key transcription factors, such as HIF and NFkB, driving aerobic glycolysis, inflammation and angiogenesis, in the tumor micro-environment.

We also identify and validate a possible mechanism for promoting oxidative stress in Cav-1 (-/-) deficient stromal cells: mitochondrial dysfunction. Experimentally, we show that Cav-1 (-/-) deficient stromal cells have (1) increased tyrosine nitration (indicative of the over-production of peroxynitrite), and that (2) the tyrosine nitration of mitochondrial complex I occurs.

Consistent with this notion, we demonstrate that Cav-1 (-/-) deficient mice have a dramatically reduced mitochondrial reserve capacity, when challenged with chemically-induced metabolic restriction with a mitochondrial complex I inhibitor (metformin) and a glycolysis inhibitor (2-deoxy-glucose). In this context, metabolic restriction is synthetically lethal with a Cav-1 deficiency. Thus, chemically-induced metabolic restriction may be a new therapeutic strategy to target Cav-1 deficient stromal cells that promote tumor growth and metastasis.

In this sense, Cav-1 (-/-) deficient mice are a new whole-body animal model for an activated lethal tumor micro-environment, i.e., "tumor stroma" without the tumor. In support of this idea, mouse mammary tumor tissue implanted in the mammary glands of Cav-1 (-/-) deficient mice results in up to a 2-fold increase in tumor growth.¹² This could explain why Cav-1 (-/-) deficient mice are tumor prone, but do not develop tumors in the absence of an epithelial-driven oncogenic stimulus.

Interestingly, in direct support of our working hypothesis, an increase in nitro-tyrosine staining in human breast cancers is associated with increased VEGF-C expression, lymph node metastasis, and poor clinical outcome (decreased recurrence-free and overall survival).¹³

Results

Rationale and transcriptional profiling data set. Loss of stromal Cav-1 expression is a powerful independent predictor of clinical outcome in human breast cancer patients, and is associated with tumor recurrence, metastasis and tamoxifen-resistance.^{7,14} To better understand these associations, we recently performed unbiased proteomic and transcriptome analysis of Cav-1 (-/-) stromal cells.¹¹ Proteomic analysis revealed the upregulation of (1) myo-fibroblast markers, (2) glycolytic enzymes and (3) anti-oxidants associated with oxidative stress.¹¹ These results were validated by immunostaining of human breast cancer samples that lack stromal Cav-1 protein expression. Similarly, transcriptional profiling provided independent support for our results from proteomic analysis.¹¹

To better understand the molecular signaling pathways that are dys-regulated in Cav-1 (-/-) stromal cells, we have now systematically re-interrogated this previously published transcriptional profiling data by subjecting it to a detailed informatics analysis.

In this data set,¹¹ if we use a lower bound cut-off of 2.0 for fold-change, 1,249 genes were upregulated and, if we use an upper bound cut-off of 0.5 for fold-change, 800 genes were downregulated in Cav-1 (-/-) stromal cells ($p \leq 0.05$). Similarly, if we use a lower bound cut-off of 1.5 for fold-change, then 4,981 genes were upregulated and, if we use an upper bound cut-off of 0.75, 4,188 genes were downregulated in Cav-1 (-/-) stromal cells ($p \leq 0.05$). Since such a large number of genes showed altered transcriptional profiles, we restricted our analysis to the genes that were upregulated.

TGF β signaling and cancer associated fibroblast markers. Our previous studies have shown that Cav-1 (-/-) stromal cells exhibit activated TGF β signaling, behave like human cancer-associated

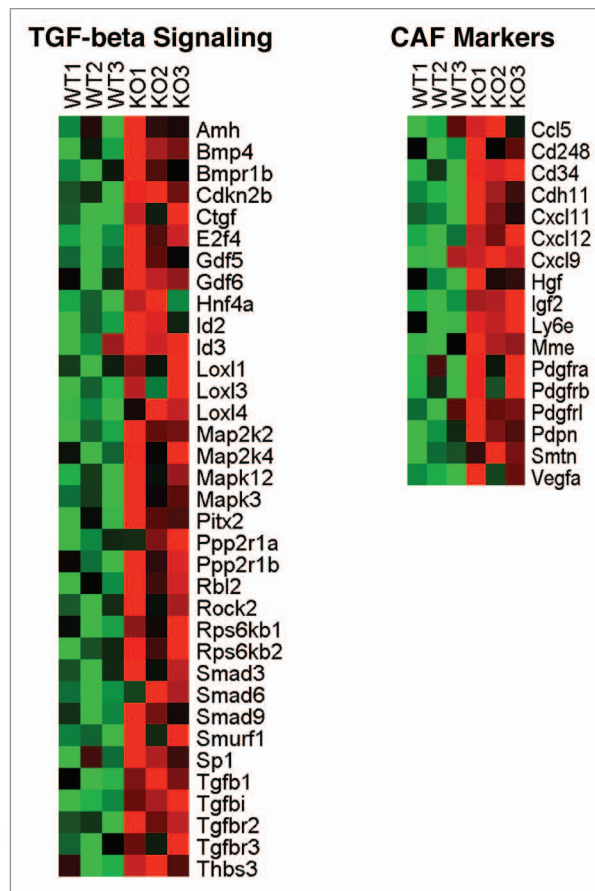


Figure 1. Heatmaps for TGF β signaling and cancer associated fibroblast markers. Cav-1 (-/-) stromal cells show the upregulation of 35 transcripts associated with activated TGF β signaling ($FC \geq 1.5$; $p \leq 0.05$; A) and the overexpression of 17 cancer-associated fibroblast markers ($FC \geq 1.5$; $p \leq 0.05$; B).

fibroblasts, and are able to induce an EMT in normal mammary epithelial cells via paracrine signaling.⁶ In accordance with these observations, Cav-1 (-/-) stromal cells show the upregulation of 35 transcripts associated with activated TGF β signaling ($FC \geq 1.5$; $p \leq 0.05$; Fig. 1A) and the overexpression of 17 cancer-associated fibroblast markers ($FC \geq 1.5$; $p \leq 0.05$; Fig. 1B).

ROS production, HIF-activation and NF κ B-activation mimic hypoxia and drive inflammation. To further simplify our analysis, we used our proteomics results as a guide for functional transcriptional analysis. Given that anti-oxidant proteins associated with oxidative stress were upregulated by proteomics in Cav-1 (-/-) stromal cells,¹¹ we first assessed the transcriptional profile of genes associated with the generation of reactive oxygen species (ROS). Interestingly, our results indicate that there are 48 genes associated with ROS-production that were upregulated in Cav-1 (-/-) stromal cells ($FC \geq 1.5$; $p \leq 0.05$). Perhaps not surprisingly, these genes are mainly associated with mitochondrial oxidative phosphorylation and peroxisome biogenesis (Fig. 2A).

ROS production is associated with the induction of aerobic glycolysis via HIF-activation and stabilization.^{15,16} This could explain our previous proteomic studies showing the upregulation of 8 glycolytic enzymes in Cav-1 (-/-) stromal cells, as many of

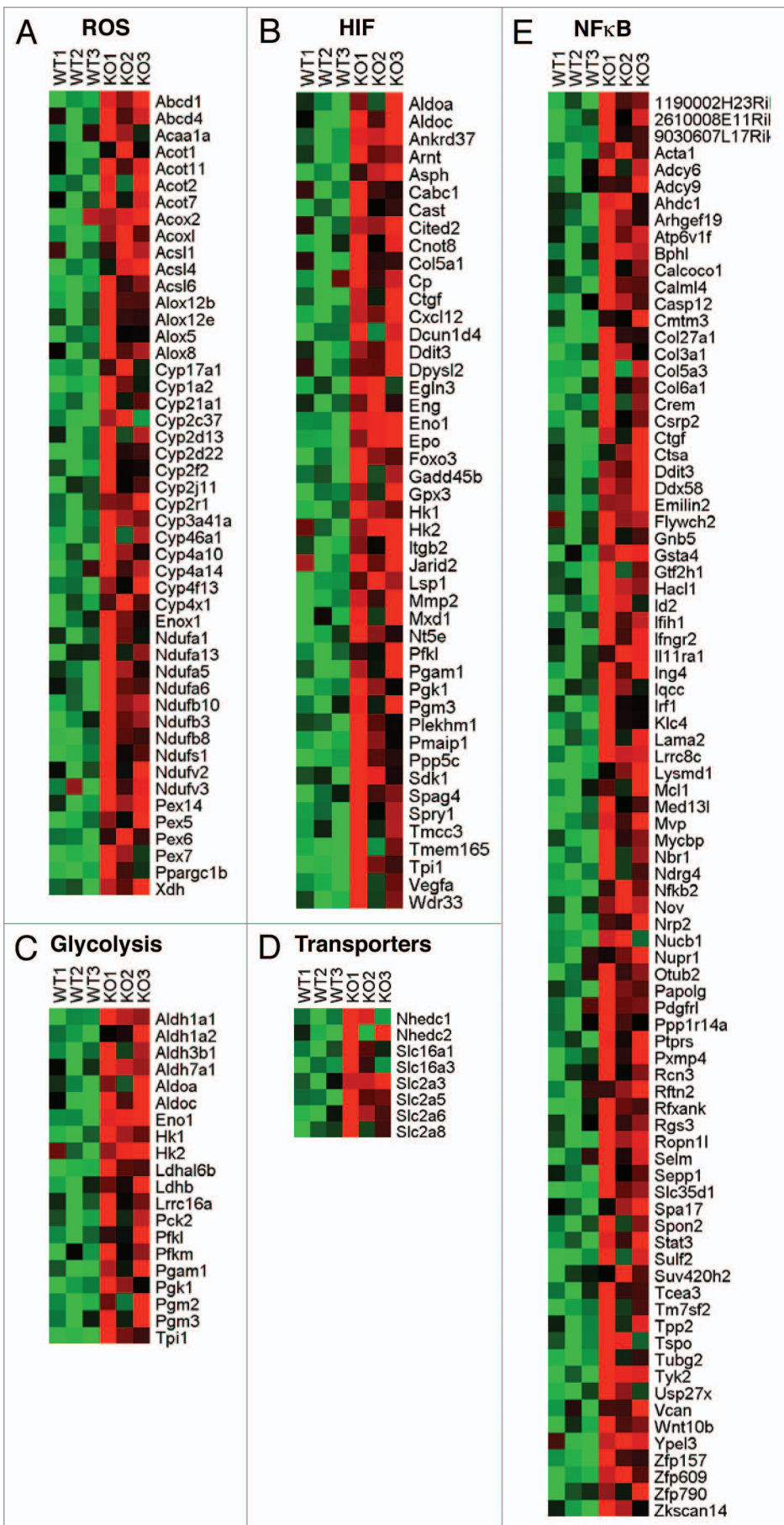


Figure 2. Heatmaps for ROS production, HIF-target genes and NFκB-activation. Cav-1 (-/-) stromal cells show the up-regulation of 48 genes associated with ROS-production ($FC \geq 1.5$; $p \leq 0.05$; A). These genes are mainly associated with mitochondrial oxidative phosphorylation (such as complex I; NADH dehydrogenase (Nduf) family members) and peroxisome biogenesis. Also, 45 known HIF-target genes were upregulated by ≥ 1.8 -fold ($p \leq 0.05$) (B). This is consistent with HIF-mediated transcriptional activation. The onset of aerobic glycolysis is supported by the induction of 21 glycolytic enzymes ($FC \geq 1.8$; $p \leq 0.05$), as well as lactate and glucose transporters (C and D). In Cav-1 (-/-) stromal cells, 86 NFκB target genes were also transcriptionally upregulated ($FC \geq 1.6$; $p \leq 0.05$).

these enzymes are HIF target genes.¹¹ Thus, we next examined the status of HIF-target genes¹⁷ in this data set. Our results show that 45 known HIF-target genes were upregulated by ≥ 1.8 -fold ($p \leq 0.05$) (Fig. 2B). This is consistent with HIF-mediated transcriptional activation. The onset of aerobic glycolysis is further supported by the induction of 21 glycolytic enzymes ($FC \geq 1.8$; $p \leq 0.05$), as well as lactate and glucose transporters (Fig. 2C and D).

ROS production also drives the inflammatory response and NFκB activation.^{16,18} As a consequence, we assessed the status of NFκB target genes¹⁹ in Cav-1 (-/-) stromal cells. Figure 2E shows that 86 NFκB target genes were transcriptionally upregulated in Cav-1 (-/-) stromal cells ($FC \geq 1.6$; $p \leq 0.05$).

Thus, we would like to propose that loss of Cav-1 in stromal cells may be mimicking hypoxia, by ROS over-production, and via the activation of HIF and NFκB target genes, thereby promoting aerobic glycolysis and inflammation in the tumor micro-environment. This Cav-1 negative stromal micro-environment, in turn, would be predicted to stimulate tumor growth and angiogenesis (Fig. 3).

Nitric oxide (NO) over-production and mitochondrial dysfunction. Given the upregulation of a number of mitochondrial genes associated with ROS production, we searched for a possible functional connection

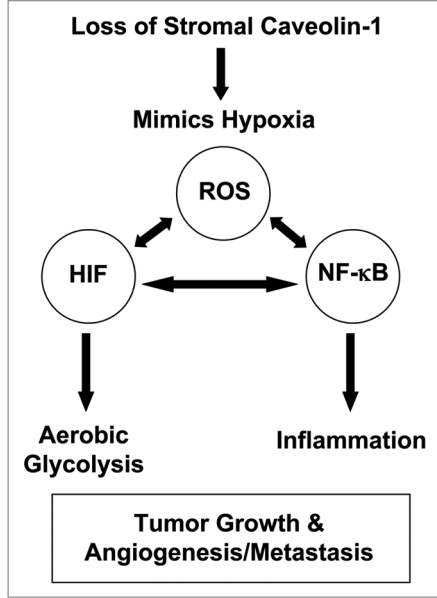


Figure 3. ROS production, HIF-activation and NF κ B-activation mimic hypoxia and drive inflammation. We propose that loss of Cav-1 in stromal cells may mimic hypoxia, by ROS over-production, and the activation of HIF and NF κ B target genes, thereby promoting aerobic glycolysis and inflammation in the tumor micro-environment. As such, the Cav-1 negative stromal micro-environment, in turn, would be predicted to stimulate tumor growth and angiogenesis.

between loss of Cav-1 expression and mitochondrial dysfunction. For example, Cav-1 is known to function as an inhibitor of eNOS, nNOS and iNOS; thus, Cav-1 (-/-) null mice show the constitutive over-production of NO species.²⁰⁻²³ NO over-production is also associated with mitochondrial dysfunction, as NO inhibits the activity of both Complex I and Complex IV (Cytochrome C Oxidase; COX),²⁴⁻³² both associated with oxidative phosphorylation. Figure 4A shows that several genes associated with NOS production and Complex IV are transcriptionally upregulated in Cav-1 (-/-) stromal cells. Similarly, Figure 2A shows that many Complex I genes are also upregulated. Thus, the transcriptional upregulation of (1) NADH dehydrogenase (Ndut) and (2) Cox genes probably represents a compensatory upregulation in response to NO-induced mitochondrial dysfunction/inhibition.

ROS, PARP, the DNA damage response and oxidative stress. ROS production is also associated with the DNA damage response, and can induce PARP proteins.³³⁻³⁵ PARPs can then serve as co-factors for the activation of a number of transcription factors, including HIF, NF κ B and AP-1.³⁶ In accordance with AP-1 activation, a number of pro-proliferative genes are also upregulated in Cav-1 (-/-) stromal cells (Fig. 5). Thus, the induction of PARP isoforms, via ROS, could explain the co-activation of these 3 transcription factors in Cav-1 (-/-) stromal cells. Figure 4B shows the upregulation of 5 PARP genes and 2 DNA-damage induced transcripts, in Cav-1 (-/-) stromal cells.

Thus, we would propose that Cav-1 (-/-) stromal cells are undergoing oxidative stress, which is inducing the DNA-damage/repair response. In accordance with this hypothesis, Cav-1 (-/-)

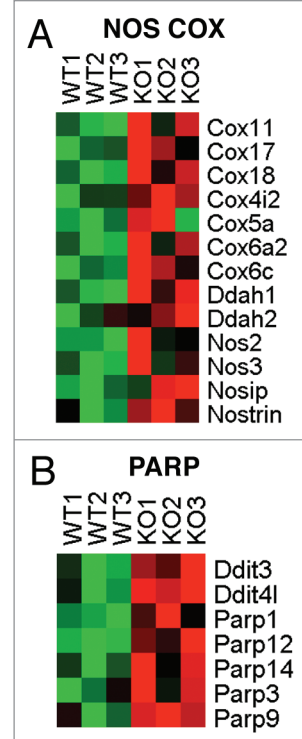


Figure 4. Heatmaps for nitric oxide (NO) and PARP signaling. Note that several genes associated with NOS production and Complex IV are transcriptionally upregulated in Cav-1 (-/-) stromal cells (A). The transcriptional upregulation of Cox genes probably represents a compensatory upregulation in response to NO-induced inhibition. ROS production is also associated with the DNA damage response, and can induce PARP proteins. PARPs can then serve as co-factors for the activation of a number of transcription factors, including HIF, NF κ B and AP-1. Thus, the induction of PARP isoforms, via ROS, could explain the co-activation of these 3 transcription factors in Cav-1 (-/-) stromal cells. (B) Shows the upregulation of 5 PARP genes and 2 DNA-damage induced transcripts, in Cav-1 (-/-) stromal cells.

stromal cells show the upregulation of 55 genes associated with the response to oxidative stress ($p < 0.05$) (GO_0006979; Fig. 6A). Similarly, Cav-1 (-/-) stromal cells show the upregulation of 129 genes associated with the DNA-damage/repair response (Fig. 6B; FC ≥ 1.6 ; $p \leq 0.05$).

Mitochondrial biogenesis and/or Dys-function. In our analysis, we also noticed that a plethora of mitochondria-associated genes were upregulated. Figure 7 shows that 151 mitochondria-associated genes were upregulated in Cav-1 (-/-) stromal cells (GO_0005739; FC ≥ 1.5 ; $p \leq 0.05$). This also includes a number of transcription factors that are known to stimulate the upregulation of mitochondrial-associated genes (Fig. 7; see inset).

A more detailed analysis revealed that Cav-1 (-/-) stromal cells have a profile of mitochondrial gene transcripts that are more characteristic of brown fat mitochondria,³⁷ especially during the thermogenic response to cold-stress (Fig. 8; compare A-C). Consistent with these observations, we see the upregulation of transcripts encoding the mitochondrial uncoupling proteins (Ucp2 and Ucp3; Figs. 6 and 7) in Cav-1 (-/-) stromal cells, which have been previously implicated

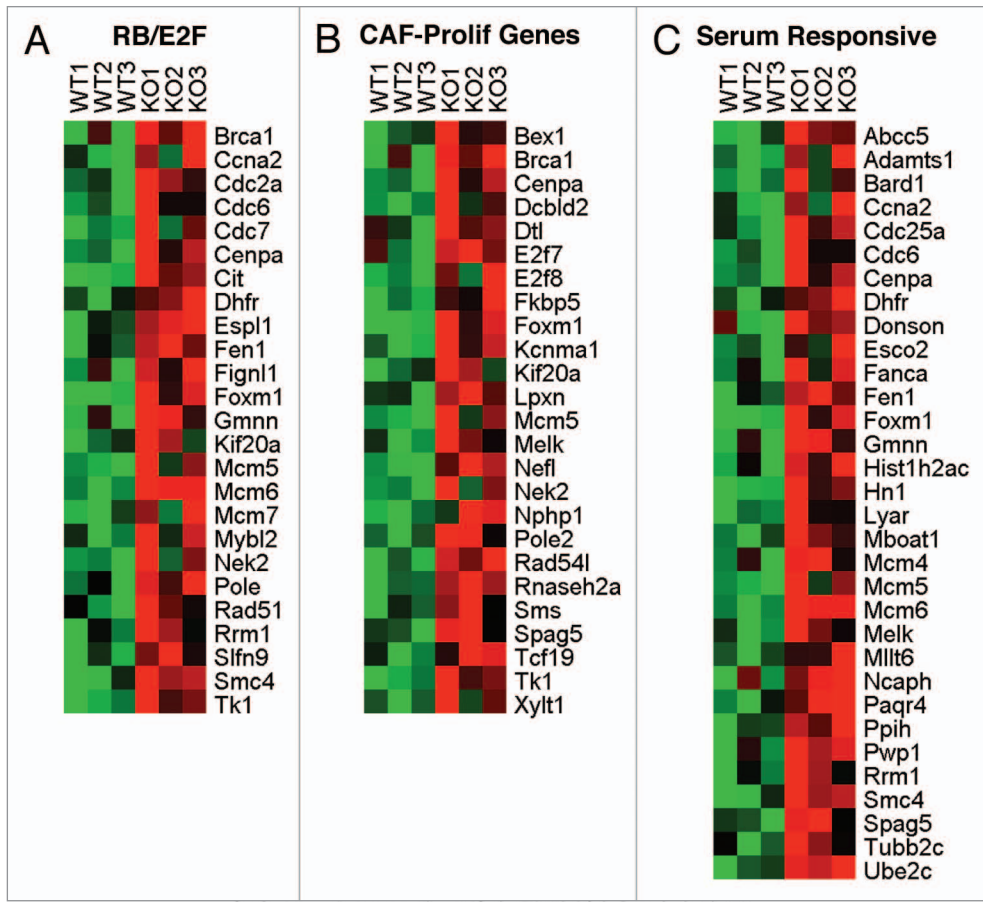


Figure 5. Heatmaps of genes associated with the proliferative response. A number of pro-proliferative genes are also upregulated in Cav-1 (-/-) stromal cells. (A) RB/E2F,⁶ (B) genes associated with the proliferation of human cancer associated fibroblasts,⁵ (C) serum responsive genes.

in driving the Warburg effect (aerobic glycolysis) in cancer cells.^{38,39}

Thus, we believe that the upregulation of mitochondria-associated genes is a compensatory response to mitochondrial dysfunction in Cav-1 (-/-) stromal cells.

The transcriptional profile of Cav-1 (-/-) stromal cells shares similarities with inflammatory signaling, stem cells, aging and neuro-degeneration. If we compare the transcriptional profile of Cav-1 (-/-) stromal cells to other existing data sets, we observe significant intersections with a number of seemingly diverse cellular processes (Table 1). As predicted, we see significant associations/overlap with oxidative stress, hypoxia, HIF- and NFκB target genes, E2F-regulated proliferative genes, as well as DNA damage and repair.

However, the four strongest associations are with (1) inflammatory signaling in myelodysplastic syndrome and acute myeloid leukemia (AML) ($p = 1.6 \times 10^{-19}$); (2) Alzheimer's disease brain ($p = 2.6 \times 10^{-18}$); (3) stem cells ($p = 1.2 \times 10^{-12}$); and (4) interferon/STAT signaling cells ($p = 2.1 \times 10^{-11}$). The similarity with genes upregulated by inhibition of DNA methylation (with 5-aza-2'-deoxycytidine (DAC)) is also consistent with an increase in "stemness" ($p = 1.8 \times 10^{-10}$) (see Table 1; Figs. 9 and 10). Venn diagrams for the transcriptional intersection

between Cav-1 (-/-) stromal cells and Alzheimer's disease are shown (Fig. 11).

We also see strong associations with breast cancer data sets, especially with ER-negative tumors ($p = 9.0 \times 10^{-10}$). IL6/STAT signaling, which has been implicated in cancer-associated fibroblast autocrine and paracrine signaling, appears to be activated ($p = 2.1 \times 10^{-10}$) (Fig. 9E).

Strong similarities with graft-versus-host disease (GVHD) are observed ($p = 1.3 \times 10^{-8}$). Interestingly, GVHD is an animal model for scleroderma and GVHD patients often develop a scleroderma-like syndrome (Fig. 9C). These observations are consistent with the idea that scleroderma fibroblasts and cancer-associated fibroblasts both share a constitutive myo-fibroblastic phenotype.

We also see associations with defective adipocyte differentiation due to IRS-1 gene deletion ($p = 1.1 \times 10^{-4}$). Interestingly, Cav-1 (-/-) deficient mice are known to have defects in adipocyte differentiation,⁴⁰ and are deficient in IRS-1 protein expression, as Cav-1 expression is required to stabilize IRS-1, by preventing its degradation.⁴¹ Thus, the cancer-associated fibroblast phenotype may somehow be related to a form of defective adipocyte differentiation. In this regard, it is important to note that adipocyte-precursor cells are indeed fibroblasts.

Finally, the upregulation of TGFbeta signaling and muscle related genes is also observed as predicted (Table 1), consistent with a myo-fibroblastic phenotype. Interestingly, TGFbeta is known to prevent the conversion of pre-adipocytes (fibroblasts) to mature adipocytes,⁴² consist with a defect in adipocyte differentiation.

Validating the role of loss of stromal Cav-1 in promoting tyrosine nitration. In order to test the hypothesis that loss of Cav-1 drives the accumulation of nitro-tyrosine in Cav-1 (-/-) deficient stromal cells, these bone-marrow derived mesenchymal cells were first subjected to immunofluorescence analysis using a nitro-tyrosine specific antibody probe. Figure 12 show that nitro-tyrosine staining was more intense in Cav-1 (-/-) deficient stromal cells, as compared with WT stromal cells processed in parallel, as predicted.

In order to rule out the possibility that this was due to the selection of different stromal cell populations from WT and Cav-1 (-/-) deficient mice, we acutely downregulated Cav-1 expression in a human fibroblast cell line (hTERT-BJ1 cells), using an siRNA approach with oligonucleotides (Cav-1 siRNA versus Control siRNA). Figure 13 shows that this siRNA approach using transiently transfected human fibroblasts successfully knocked-down Cav-1 expression, resulting the accumulation of nitro-tyrosine species. Thus, acute loss of Cav-1 in stromal fibroblasts is associated with the over-production of NO and tyrosine nitration.

To determine if mitochondrial components of the respiratory chain might be one of the targets of tyrosine nitration, we used a well-characterized approach via immunoprecipitation to immuno-capture mitochondrial complex I from whole cell lysates. These immunoprecipitates were then subjected to Western blot analysis to detect the presence of nitro-tyrosine in mitochondrial complex I components.

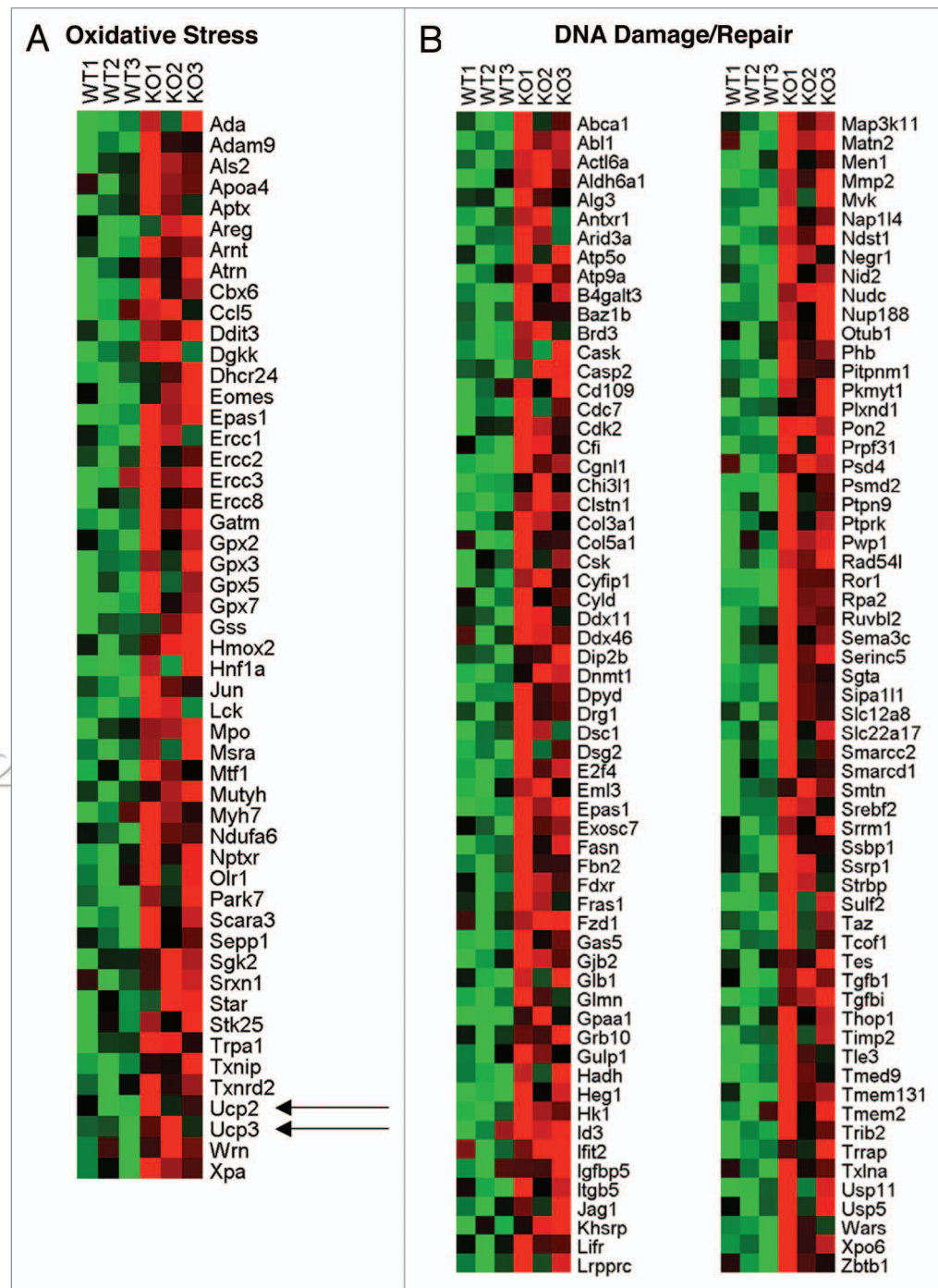


Figure 6. Heatmaps of genes related to oxidative stress and DNA damage/repair. Here, we propose that Cav-1 (-/-) stromal cells are undergoing oxidative stress, which is inducing the DNA-damage/repair response. In accordance with this hypothesis, Cav-1 (-/-) stromal cells show the upregulation of 55 genes associated with the response to oxidative stress ($p \leq 0.05$) (A). Similarly, Cav-1 (-/-) stromal cells show the upregulation of 129 genes associated with the DNA-damage/repair response ($FC \geq 1.6$; $p \leq 0.05$; B).

Figure 14 shows that nitro-tyrosine selectively accumulated in a >225 kDa component of mitochondrial complex I, and tyrosine nitration was dramatically increased in the absence of Cav-1. Virtually identical results were obtained with both Cav-1 (-/-) deficient stromal cells and fibroblasts transiently transfected with Cav-1 siRNA, processed in parallel.

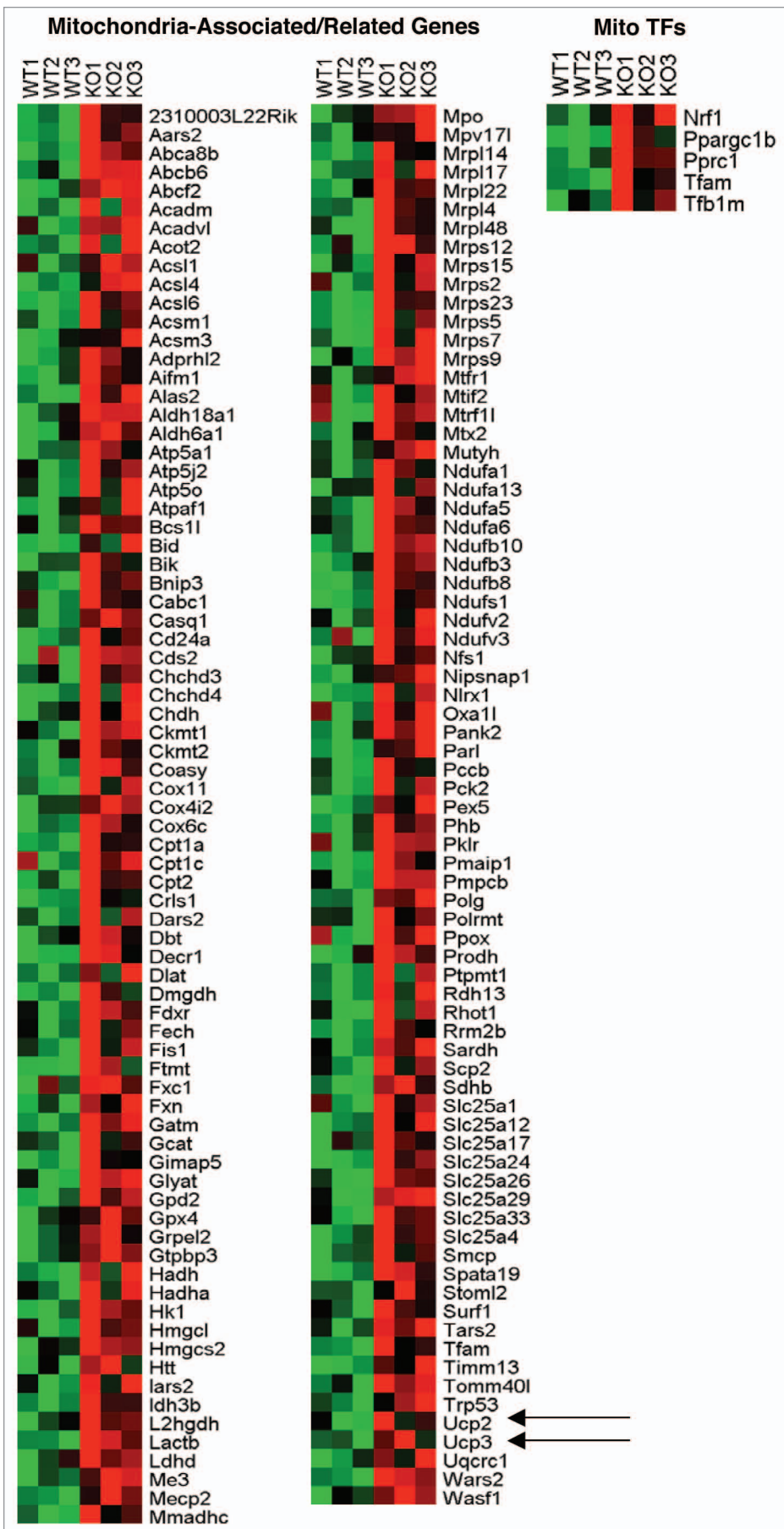


Figure 7. Heatmaps of genes associated with mitochondrial biogenesis and/or dysfunction. We noticed that a plethora of mitochondria-associated genes were upregulated. Note that 151 mitochondria-associated genes were upregulated in Cav-1 (-/-) stromal cells ($\text{FC} \geq 1.5$; $p \leq 0.05$). This also includes a number of transcription factors that are known to stimulate the upregulation of mitochondrial-associated genes (see inset).

Thus, loss of Cav-1 may result in the inactivation of mitochondrial complex I via tyrosine nitration.

Validating the role of loss of Cav-1 in mitochondrial dysfunction: chemically-induced metabolic restriction reveals a reduction in mitochondrial reserve capacity in Cav-1 (-/-) deficient mice. Next, we determined if Cav-1 mice are more susceptible to metabolic restriction with mitochondrial and glycolysis inhibitors. We reasoned that if Cav-1 (-/-) deficient mice suffer from mitochondrial dysfunction, then they will have a reduced mitochondrial reserve capacity. For this purpose, we used metformin (a mitochondrial complex I inhibitor) and 2-DG (2-deoxyglucose; a glycolysis inhibitor).

For this purpose, WT and Cav-1 (-/-) deficient mice were starved for 4 hours, and injected (i.p.) with metformin (300 mg/kg/day) or 2-DG (500 mg/kg/day), either individually or in combination.

Interestingly, administration of metformin or 2-DG individually did not seriously affect the WT or Cav-1 (-/-) deficient mice, all of which quickly recovered.

However, the combination of metformin and 2-DG in Cav-1 (-/-) deficient mice was lethal (Fig. 15). Eighty-percent of the Cav-1 (-/-) deficient mice injected died on day 1, and 100% died by day 2 ($p < 0.0008$). In striking contrast, WT mice injected daily with the combination (Met + 2-DG) were followed for at least 13 days, and showed no deaths.

Thus, it appears that (1) Cav-1 (-/-) deficient mice have a reduced mitochondrial reserve capacity, and 2) that metabolic restriction with chemical inhibitors is synthetically lethal with a Cav-1 (-/-) deficiency.

These findings have important implications for blocking the “reverse Warburg effect” in human breast cancer patients, which show a loss of stromal Cav-1.

Discussion

Here, we used an informatics analysis of genome-wide transcriptional profiling data obtained from WT and Cav-1 (-/-) deficient stromal cells, to identify the major signaling pathways and transcriptional programs that are activated by a stromal Cav-1 deficiency. Our informatics results suggest that a loss of stromal Cav-1 drives oxidative stress, mimics hypoxia, and increases inflammation in the tumor microenvironment, via increased NO production, HIF- and NF κ B activation, and mitochondrial dysfunction (Fig. 16). Increased NO production in Cav-1 (-/-) mice and endothelial cells derived from these animals is well documented,²⁰ as Cav-1 normally directly interacts with eNOS, nNOS and iNOS, and tonically inhibits their activity.⁴³ Similarly, others have shown that endothelial cells derived from Cav-1 (-/-) null animals show increased NO and ROS production.²³ Thus, our observation that Cav-1 (-/-) deficient fibroblasts show an accumulation of tyrosine nitration is consistent with these previous experimental findings. However, tyrosine nitration of mitochondrial complex I was not previously evaluated in Cav-1 (-/-) null animals or cells. Thus, NO over-production in Cav-1 (-/-) mice may have dire consequences for mitochondrial function, leading to more oxidative stress.

In support of this notion, we show here that metabolic restriction with a mitochondrial complex I inhibitor (metformin) and a glycolysis inhibitor (2-deoxy-glucose) is synthetically lethal with a Cav-1 deficiency in whole animals. Under these conditions, 80% of the Cav-1 null mice died within 1 day of treatment, and 100% died within 2 days of treatment, while WT mice did not show any lethality (or serious impairment) for up to 13 days of treatment. Thus, experimentally, Cav-1 deficient mice suffer from a reduced mitochondrial reserve capacity. As such, chemically-induced metabolic restriction may be a new therapeutic strategy to target

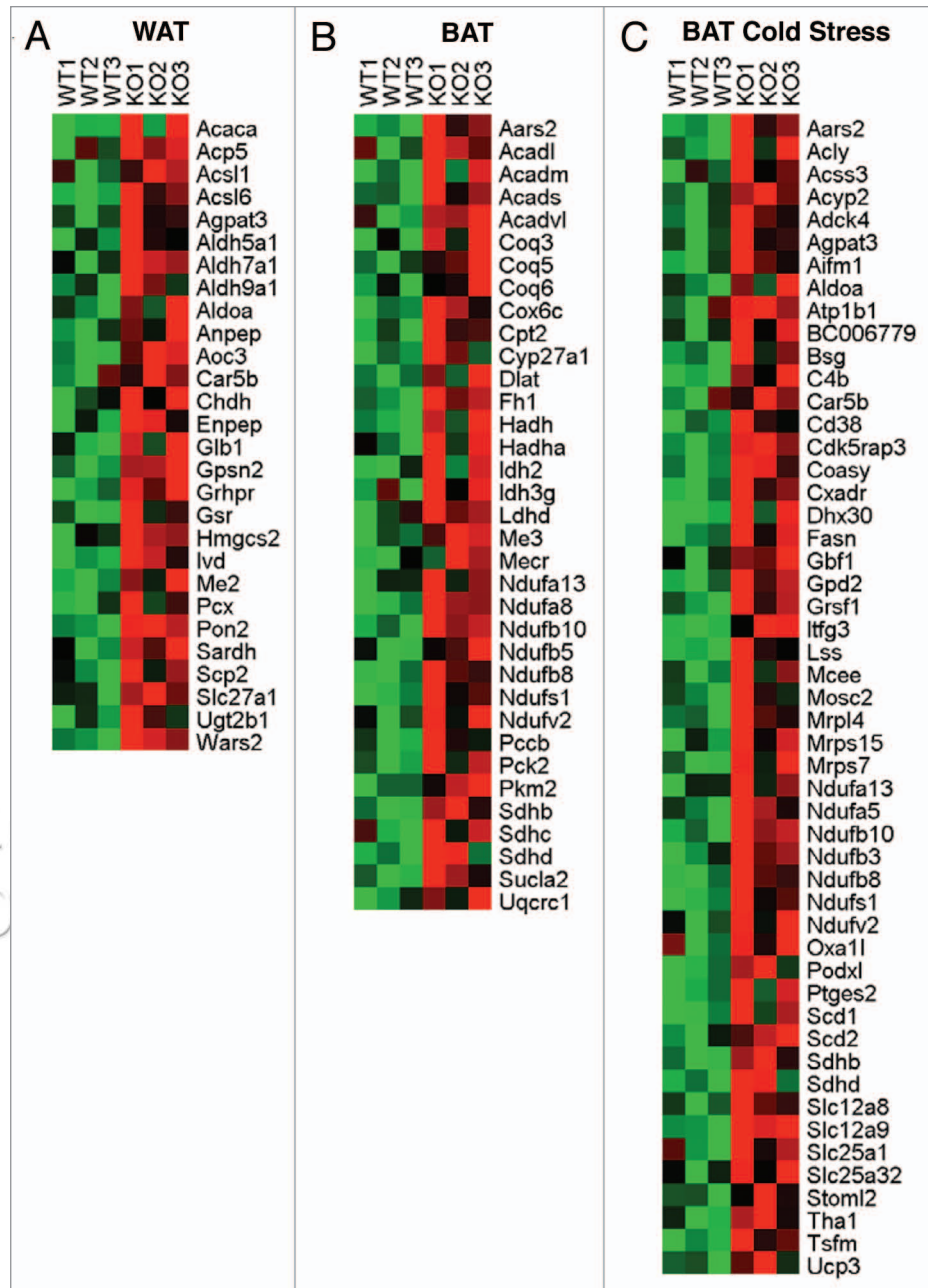


Figure 8. Heatmaps of genes associated with brown- and white-adipose tissue mitochondria. Cav-1 (-/-) stromal cells have a profile of mitochondrial gene transcripts that are more characteristic of brown fat mitochondria, especially during the thermogenic response to cold-stress (B; compare panels A–C). Consistent with these observations, we see the upregulation of transcripts encoding the mitochondrial uncoupling proteins (Ucp2 and Ucp3; Figs. 6 & 7) in Cav-1 (-/-) stromal cells, which have been previously implicated in driving the Warburg effect (aerobic glycolysis) in cancer cells. Thus, the upregulation of mitochondria-associated genes may be a compensatory response to mitochondrial dysfunction in Cav-1 (-/-) stromal cells. WAT, white adipose tissue; BAT, brown adipose tissue.

Cav-1 deficient stromal cells that promote tumor growth and metastasis in a paracrine fashion (the “reverse Warburg effect”).

Importantly, in direct support of our hypothesis, an increase in nitro-tyrosine staining in human breast cancers is associated with increased VEGF-C expression, lymph node metastasis, and poor clinical outcome (decreased recurrence-free and overall survival).¹³

Table 1. Overlap of the Cav-1 (-/-) stromal cell upregulated data set with other existing gene data sets

Data Set	Description	p-value
Myelodysplastic Syndrome and Acute Myeloid Leukemia		
TAKEDA_NUP8_HOXA9_10D_UP	Effect of NUP98-HOXA9 on gene transcription at 10 d after transduction UP	1.63E-19
TAKEDA_NUP8_HOXA9_3D_UP	Effect of NUP98-HOXA9 on gene transcription at 3 d after transduction UP	1.01E-16
Aging and Neurodegenerative Disorders		
ALZHEIMERS_DISEASE_UP	Upregulated in correlation with overt Alzheimer's Disease, in the CA1 region of the hippocampus	2.55E-18
AGED_MOUSE_NEOCORTEX_UP	Upregulated in the neocortex of aged adult mice (30-month) vs. young adult (5-month)	7.76E-05
Stem Cells		
STEMCELL_HEMATOPOIETIC_UP	Enriched in mouse hematopoietic stem cells, compared to differentiated brain and bone marrow cells	1.18E-12
BYSTRYKH_HSC_TRANS_GLOCUS	Trans-regulated hematopoietic stem cell (HSC) transcripts detected in bone marrow tissue (high likelihood ratio statistic (LRS) value and genome-wide linkage p < 0.005) marrow and fetal liver (ST-HSC Shared)	2.64E-10
Interferon/STAT Signaling		
DAC_IFN_BLADDER_UP	Interferon-regulated genes upregulated by DAC treatment in T24 bladder carcinoma cells	2.07E-11
GRANDVAUX_IFN_NOT_IRF3_UP	Genes upregulated by interferon-alpha, beta but not by IRF3 in Jurkat (T cell)	5.11E-09
Actin Cytoskeleton and Cell Movement; Muscle Related Genes		
ACTIN_FILAMENT_BASED_PROCESS	Genes annotated by the GO term GO:0030029. Any cellular process that depends upon or alters the actin cytoskeleton, that part of the cytoskeleton comprising actin filaments and their associated proteins.	4.35E-11
CELL_PROJECTION	Genes annotated by the GO term GO:0042995. A prolongation or process extending from a cell, e.g., a flagellum or axon.	3.77E-07
Inhibition of DNA Methylation		
DAC_BLADDER_UP	Upregulated by DAC treatment in T24 bladder carcinoma cells	1.75E-10
TSA_RKO_UP	Upregulated by TSA alone, with non-hypermethylated promoters, in RKO cells	1.10E-02
IL-6/STAT Signaling		
IL6_FIBRO_UP	Upregulated following IL-6 treatment in normal skin fibroblasts	2.05E-10
IL6_SCAR_FIBRO_UP	Upregulated following IL-6 treatment in hypertrophic scar fibroblasts	2.92E-09
Breast Cancer Associated Genes		
BRCA_ER_NEG	Genes whose expression is consistently negatively correlated with estrogen receptor status in breast cancer—higher expression is associated with ER-negative tumors	8.96E-10
BRCA_ER_POS	Genes whose expression is consistently positively correlated with estrogen receptor status in breast cancer—higher expression is associated with ER-positive tumors	2.77E-03
Graft-Versus-Host Disease		
ICHIBA_GVHD	Genes whose expression is altered greater than twofold in mouse livers experiencing graft-versus-host disease (GVHD) as a result of allogenic bone marrow transplantation	1.33E-08
Viral Infection		
CMV_HCMV_TIMECOURSE_12HRS_UP	Upregulated in fibroblasts following infection with human cytomegalovirus (at least 3-fold, with Affymetrix change call, in at least two consecutive timepoints), with maximum change at 12 hours	9.90E-08
RIBAVIRIN_RSV_UP	Upregulation by infection of human pulmonary epithelial cells (A549) with respiratory syncytial virus (RSV) is enhanced by the anti-viral drug ribavirin	6.16E-07
NFkappaB Signaling		
TNFALPHA_ADIP_UP	Upregulated in mature, differentiated adipocytes following treatment with TNFalpha	5.08E-07
V\$NFKAPPAB_01	Genes with promoter regions [-2 kb, 2 kb] around transcription start site containing the motif GGGAMTTYCC which matches annotation for NFkB	4.92E-03
TGFbeta Signaling		
TGFBETA_C4_UP	Upregulated by TGFbeta treatment of skin fibroblasts, cluster 4	9.78E-06

For this overlap analysis, UP genes from the Cav-1 (-/-) stromal data set with a fold-change of ≥ 2.0 (KO/WT) and a p value of ≤ 0.1 were utilized for comparison with existing gene sets in the data base. Only two representative gene sets are shown for each category. For a more complete list of intersecting gene sets, see **Supplemental Table 3**.

Table 1. Overlap of the Cav-1 (-/-) stromal cell upregulated data set with other existing gene data sets (continued).

EMT_UP	Upregulated during the TGFbeta-induced epithelial-to-mesenchymal transition (EMT) of Ras-transformed mouse mammary epithelial (Eph4) cells (EMT is representative of late-stage tumor progression and metastasis)	9.03E-03
IL-4/STAT Signaling		
IL4PATHWAY	IL-4 promotes Th2 cell differentiation via a heterodimeric receptor that activates Stat6/JAK and MAP kinase pathways.	1.97E-05
Vasculogenesis and Angiogenesis		
VASCULATURE_DEVELOPMENT	Genes annotated by the GO term GO:0001944. The process whose specific outcome is the progression of the vasculature over time, from its formation to the mature structure.	9.50E-05
ANGIOGENESIS	Genes annotated by the GO term GO:0001525. Blood vessel formation when new vessels emerge from the proliferation of pre-existing blood vessels.	9.25E-04
Defective Adipocyte Differentiation		
IRS1_KO_ADIP_UP	Upregulated in brown preadipocytes from Irs1-knockout mice, which display severe defects in adipocyte differentiation, versus wild-type controls	1.07E-04
E2F Regulated/Cell Proliferation Genes		
V\$E2F1DP1_01	E2F regulated Genes	1.12E-04
V\$E2F1DP2_01	E2F regulated Genes	1.12E-04
Stress Response		
RESPONSE_TO_STRESS	Genes annotated by the GO term GO:0006950. A change in state or activity of a cell or an organism (in terms of movement, secretion, enzyme production, gene expression, etc.,) as a result of a stimulus indicating the organism is under stress. The stress is usually, but not necessarily, exogenous (e.g., temperature, humidity, ionizing radiation).	1.54E-04
Glycolysis, Hypoxia and HIF Target Genes		
V\$HIF1_Q3	Hif-1 (hypoxia-inducible factor 1) transcriptional targets	1.94E-04
GLYCOLYSIS	Genes involved in glycolysis	9.71E-04
Multiple Myeloma and Mixed Lineage Leukemia		
ZHAN_MULTIPLE_MYELOMA_VS_NORMAL_UP	The 70 most significantly upregulated genes in MM in comparison with normal bone marrow PCs	3.64E-04
SCHRAETS_MLL_UP	Expression profile of MLL versus wild-type cells	3.77E-03
Mitochondria and Fatty Acid Metabolism/Oxidation		
FATTY_ACID_METABOLISM	Fatty Acid Metabolism	4.12E-03
FATTY_ACID_BETA_OXIDATION	Genes annotated by the GO term GO:0006635. The metabolic oxidation of a long-chain fatty acid by successive cycles of reactions during each of which the fatty acid is shortened by a two-carbon fragment removed as acetyl coenzyme A	7.83E-03
DNA Damage and Repair		
MORF_RPA2	Neighborhood of RPA2 replication protein A2, 32 kDa in the MORF expression compendium	1.21E-03
BAF57_BT549_UP	Upregulated following stable re-expression of BAF57 in Bt549 breast cancer cells that lack functional BAF57	8.66E-03

For this overlap analysis, UP genes from the Cav-1 (-/-) stromal data set with a fold-change of ≥ 2.0 (KO/WT) and a p value of ≤ 0.1 were utilized for comparison with existing gene sets in the data base. Only two representative gene sets are shown for each category. For a more complete list of intersecting gene sets, see **Supplemental Table 3**.

A decrease in mitochondrial reserve capacity is consistent with our previous functional and morphological studies, showing that Cav-1 null mice have mitochondrial abnormalities.⁴⁴ For example, we showed that in skeletal muscle, Cav-1 null mice develop tubular and mitochondrial aggregates, with increased satellite cell numbers, consistent with repeated injury and continuous regeneration.⁴⁵ Similarly, in white adipose tissue, we noted that Cav-1 null mice show the mis-localization of mitochondria, which are no longer embedded within the lipid droplet membrane.⁴⁶ This was functionally correlated with a defect both in lipid accumulation and triglyceride hydrolysis, leading to defects in hormonally-regulated increases in free fatty acids.⁴⁶ We also

evaluated mitochondrial status in brown adipose tissue, which is related to thermo-regulation. Interestingly, under conditions of metabolic restriction (by food removal) and cold treatment, Cav-1 null mice failed to maintain their body temperature and became obtunded.⁴⁷ Again, this appeared to be due to a defect in the liberation of free fatty acids, as well as a defect in fatty acid beta-oxidation, as assessed by a reduction in AMP-kinase activation in Cav-1 null mice.⁴⁷ Electron microscopy revealed dramatic perturbations in the mitochondria of Cav-1 (-/-) null interscapular brown adipocytes. More specifically, mitochondria from Cav-1 (-/-) brown fat adipocytes were larger, dilated, and much less electron dense than the mitochondria of wild-type

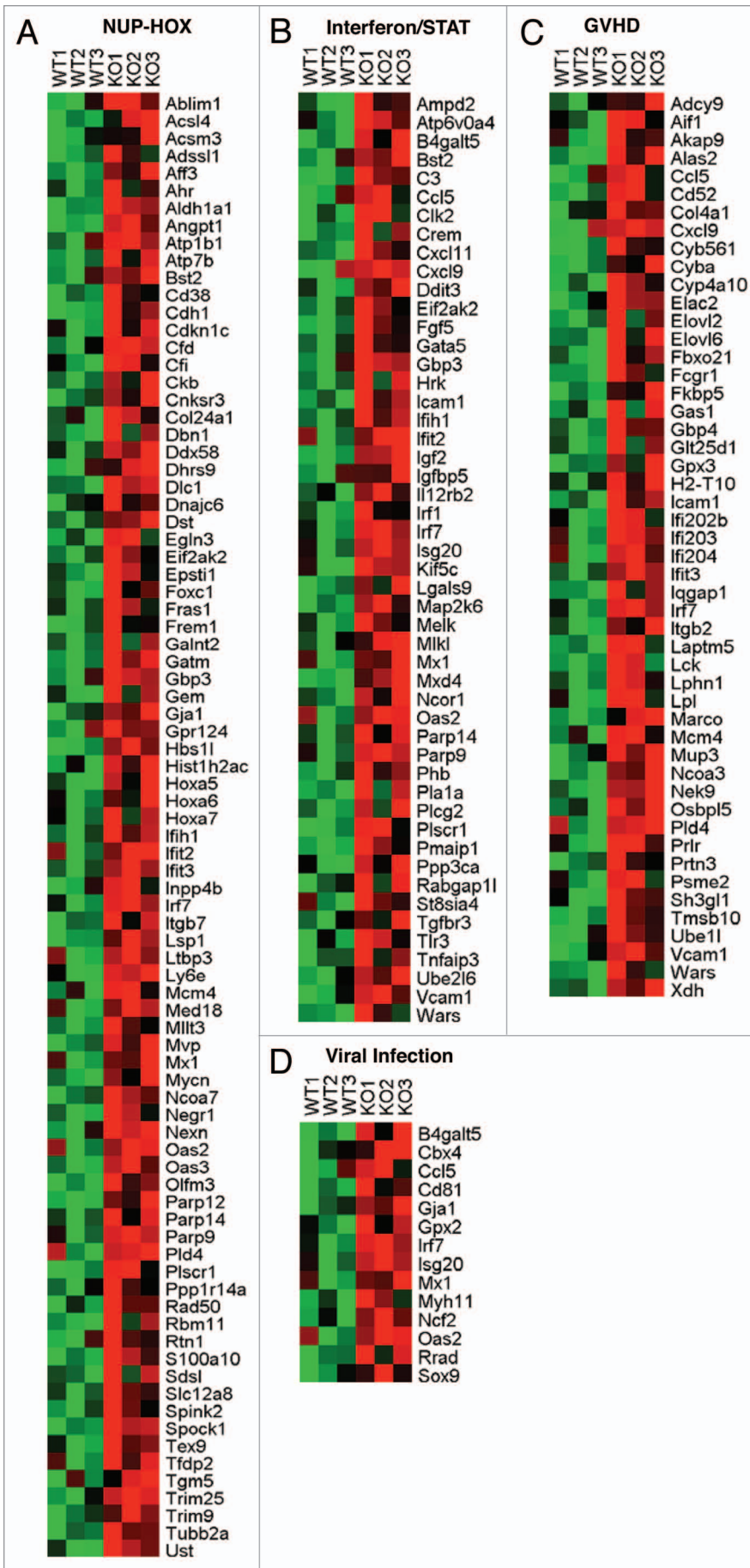


Figure 9. Heatmaps of genes associated with inflammatory signaling. When we compare the transcriptional profile of Cav-1 (-/-) stromal cells to other existing data sets, we observe significant intersections with a number of seemingly diverse cellular processes (Table 1). These include (A) inflammatory signaling in myeloid-plastic syndrome and acute myeloid leukemia (AML) ($p = 1.6 \times 10^{-19}$); and (B) interferon/STAT signaling cells ($p = 2.1 \times 10^{-11}$). Strong similarities with graft-versus-host disease (GVHD) ($p = 1.3 \times 10^{-8}$) (C) and viral infection ($p = 9.9 \times 10^{-8}$) (D), as well as IL-6 signaling ($p = 2.1 \times 10^{-10}$).

mice.⁴⁷ Thus, these previous results all point towards mitochondrial dysfunction, and a reduced mitochondrial reserve capacity.

Relevant complementary studies were also performed by Pol and colleagues.⁴⁸ In their studies, they showed that a Cav-1 deficiency was synthetically lethal with a partial hepatectomy.⁴⁸ Interestingly, this lethality could be rescued if Cav-1 null mice were fed glucose, but not fatty acids.⁴⁸ This finding is consistent with the idea that Cav-1 deficient mice are strictly dependent on glucose for energy metabolism (via aerobic glycolysis). These data are also consistent with the idea that Cav-1 null mice may suffer from a defect in mitochondrial beta-oxidation.⁴⁰ Similarly, we have shown that Cav-1 null mice have elevated post-prandial triglyceride levels and elevated post-prandial free fatty acid levels, so this may reflect their inability to properly store fatty acids and an inability to use them as an energy source, via mitochondrial beta-oxidation.⁴⁰ This would also explain the ~3–4-fold increase in brown fat mass observed in Cav-1 null mice, a possible compensatory response to mitochondrial dysfunction and/or hyper-triglyceridemia.⁴⁰

Implications for the fibrotic disease spectrum: scleroderma, keloid formation, pulmonary fibrosis and post-surgical adhesions. The major signaling pathways that we have identified here as activated in Cav-1 (-/-) null bone marrow-derived stromal cells (a.k.a. mesenchymal stem cells), such as increased ROS production, HIF-activation and NF κ B activation, may also have implications for understanding the pathogenesis of several fibrotic diseases, such as scleroderma (systemic sclerosis) and pulmonary fibrosis, as well as keloid (scar) formation. In fact, Cav-1 (-/-) deficient mice have already been shown to have a pro-fibrotic phenotype, and have been used as a mouse model for scleroderma and pulmonary fibrosis.^{49–52}

In accordance with this assertion, ROS over-production, constitutive activation of HIF and NF κ B, have all been implicated in the pathogenesis of pro-fibrotic diseases, including scleroderma, keloid formation and pulmonary fibrosis.⁵³⁻⁷⁵

Thus, our current results further validate the use of Cav-1 (-/-) mice as a general model for pro-fibrotic disease. As such, any therapies that are identified that selectively target Cav-1 (-/-) fibroblasts or Cav-1 (-/-) mesenchymal stem cells could be used to combat both (i) tumor growth and metastasis, as well as (ii) tissue fibrosis (including scleroderma, keloid formation, pulmonary fibrosis, cardiac fibrosis and post-surgical adhesions).

In fact, we show here that the transcriptional profile of Cav-1 (-/-) stromal cells is very similar to that of graft-versus-host disease (GVHD; Fig. 9), which is a frequently used animal model for fibrosis and systemic sclerosis.^{76,77} Interestingly, bone marrow transplantation is sufficient to resolve scleroderma in patients,^{78,79} and is now being explored for solid tumors, such as breast cancer.⁸⁰

Thus, pro-fibrotic disease(s) and tumor progression/metastasis may both be due to the propagation of an abnormal population of activated pro-fibrotic myo-fibroblastic mesenchymal stem cells.

Interestingly, it has recently been proposed that pulmonary arterial hypertension (PAH) and the resulting fibrosis are due to the “Warburg effect”, with a cancer-related metabolic shift towards aerobic glycolysis in pulmonary arterial smooth muscle cells.⁸¹⁻⁸³ More specifically, Archer and colleagues went on to show that therapy with dichloroacetate (DCA), which is a glycolysis inhibitor that produces a shift towards oxidative metabolism, was sufficient to reverse the Warburg-like phenotype of pulmonary arterial smooth muscle cells, preventing fibrosis and increasing survival. This shift toward aerobic glycolysis may also explain why Cav-1-deficient mice also spontaneously develop PAH and lung fibrosis.^{49,50,84,85} Similarly, we have recently shown that glycolysis inhibitors (such as DCA and 2-DG) can prevent the tumor-promoting effects of Cav-1-deficient cancer associated fibroblasts.⁸⁶

Thus, we may be able to combat both fibrotic spectrum diseases (scleroderma, keloids, pulmonary fibrosis and post-surgical adhesions) and tumor progression/metastasis, with targeted glycolytic therapy.

In fact, keloid lesions, which consist mainly of myofibroblasts and collagen, accumulate up to nearly 3-fold higher levels of 18-fluorodeoxyglucose (FDG),⁸⁷ which can be visualized by positron emission tomography (PET). As keloid myofibroblasts⁶¹ are known to undergo Warburg metabolism (aerobic glycolysis), thus we propose that FDG imaging can also be used to visualize the “reverse Warburg effect” (fibroblastic stromal glycolysis) in human tumors *in vivo*. If fact, PET imaging with FDG may be already routinely detecting the “reverse Warburg effect”, although positive signal in tumor tissue has been previously/wrongly attributed to tumor and endothelial cells and not fibroblasts.

In direct support of this notion, PET scanning with FDG is already being used extensively to clinically monitor the treatment and progression of fibrotic diseases, including pulmonary fibrosis and post-surgical scars/adhesions.⁸⁸⁻⁹⁴

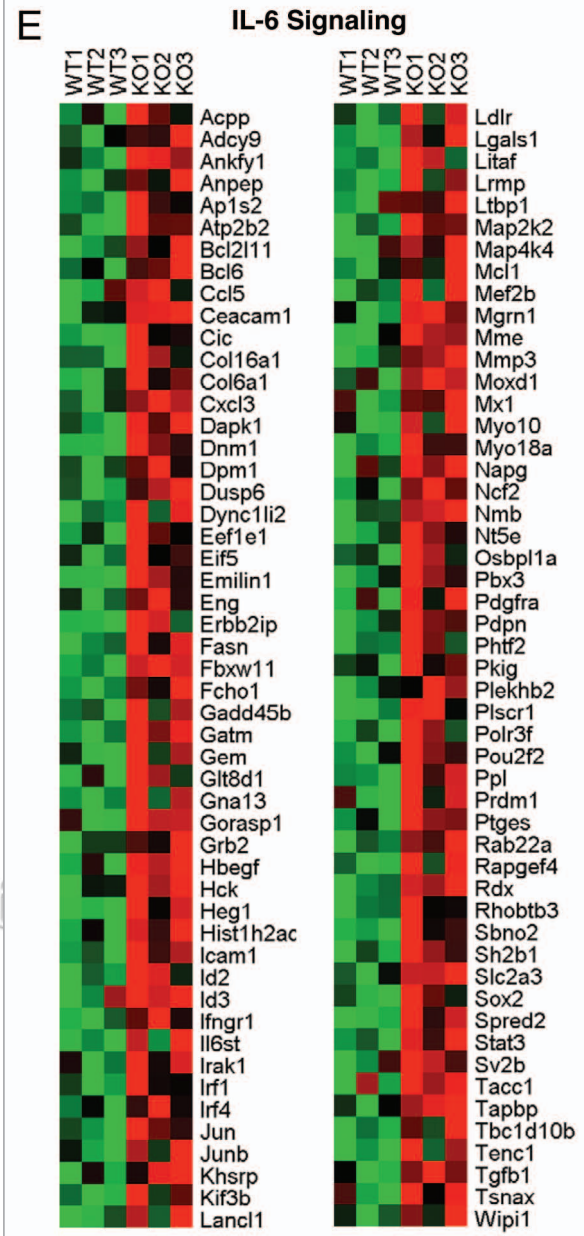


Figure 9 (continued). Heatmaps of genes associated with inflammatory signaling. When we compare the transcriptional profile of Cav-1 (-/-) stromal cells to other existing data sets, we observe significant intersections with a number of seemingly diverse cellular processes (Table 1). These include (E) IL-6 signaling.

Materials and Methods

Gene set enrichment analysis and computing gene set p-values. The Molecular Signatures Database (MsigDB⁹⁵) is a collection of gene sets:

- collected from various sources such as online pathway databases, publications, and knowledge of domain experts,
- comprising genes that share a conserved cis-regulatory motif across the human, mouse, rat and dog genomes,

Alzheimer's Disease Brain/Aging

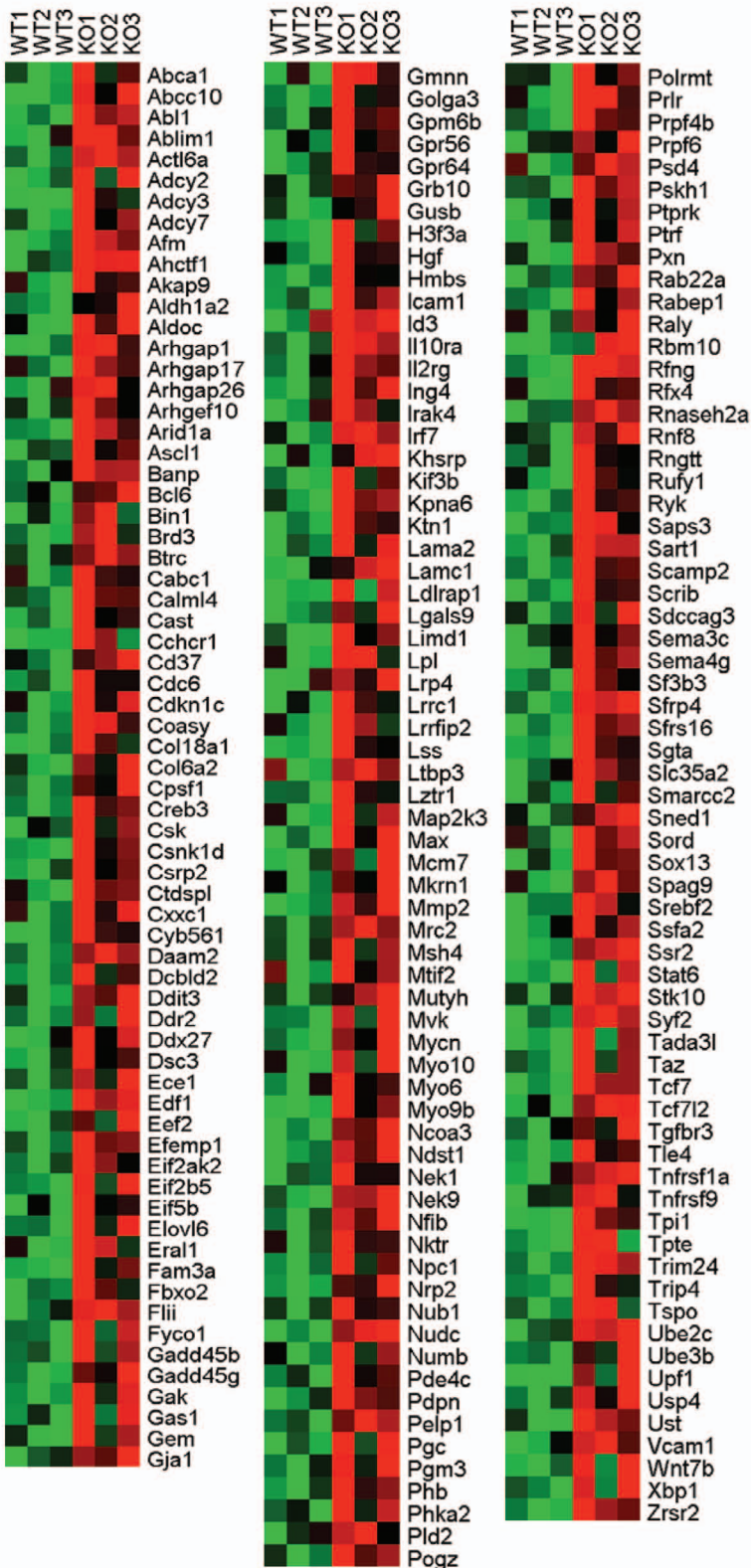


Figure 10. Heatmaps of genes associated with Alzheimer disease/aging in the brain. Remarkably, Cav-1 (-/-) stromal cells bear a striking resemblance to Alzheimer's disease brain tissue, which also functionally suffers from oxidative stress, NO over-production (peroxynitrite formation), inflammation, hypoxia and mitochondrial dysfunction ($FC \geq 1.8$; $p \leq 0.05$; overlap of 207 genes).

- identified as co-regulated gene clusters by mining large collections of cancer-oriented microarray data, and

- annotated by a common Gene Ontology (GO) term.

For our analysis we used the latest release of MSigDB database v2.5 (April 7, 2008), after converting all the gene names in the database into RefSeq gene IDs. After this preprocessing step, we chose the sub-collection of gene sets that was relevant to our study, and for each gene set X in that sub-collection, we computed the overlap between X and the set of genes Y from our experiments that showed a fold-change greater than or equal to 2.0 between Cav-1 (-/-) and wild-type stromal cells at a p-value less than or equal to 0.1. Then, we computed the probability (p-value) that the observed overlap between sets X and Y is less than or equal to the overlap between set X and a randomly-chosen set of size equal to the size of set Y. This probability was calculated by applying the cumulative density function of the hypergeometric distribution on the size of set X, the size of set Y, the observed overlap between X and Y, and the total number of available genes.

Isolation and culture of bone-marrow derived stromal cells (BMSCs). BMSCs were generated, as we previously described.¹¹ Briefly, bone marrow cells were collected from 10-week-old wild-type and Cav-1 (-/-) mice by flushing the hind leg bones (femur and tibia) with PBS. Bone marrow cells were then washed twice with PBS, and plated in 10 cm tissue culture dishes with Minimum Essential Media alpha (alpha-MEM; A10490-01, Gibco-Invitrogen), containing 10% FBS. Once the cultures reached ~80–90% confluence, cells were trypsinized and re-plated. Bone-Marrow Derived Stromal Cells (BMSCs) were used for experiments at passage 3.

siRNA treatment of hTERT-BJ1 fibroblasts. Cells were seeded to achieve ~70–80% confluence in enough volume of complete media to the cover plate. Thirty minutes later, cells were transiently transfected with siRNA oligos directed against human Cav-1 (Target sequence: AAG CAT CAA CTT GCA GAA AGA) (Qiagen Cat. # SI00299635) or control siRNA oligos (Target sequence: AAT TCT CCG AAC GTG TCA CGT) (Qiagen, Cat. # 1022076), with the Qiagen HiPerFect transfection reagent, according to manufacturer's protocol. Three hours post-transfection, cells were supplemented with 2x volume of complete media. siRNA-treated cells were used for experiments 24–36 hours post-transfection.

Immunofluorescence analysis. Cells were fixed for 30 minutes at room temperature in 2% PFA diluted in PBS, permeabilized for 10 minutes at room temperature with IF buffer (PBS supplemented with 0.1 mM CaCl₂ and 1 mM of MgCl₂ (PBS/CM), 0.2% BSA and 0.1% Triton X-100). Free aldehydes groups

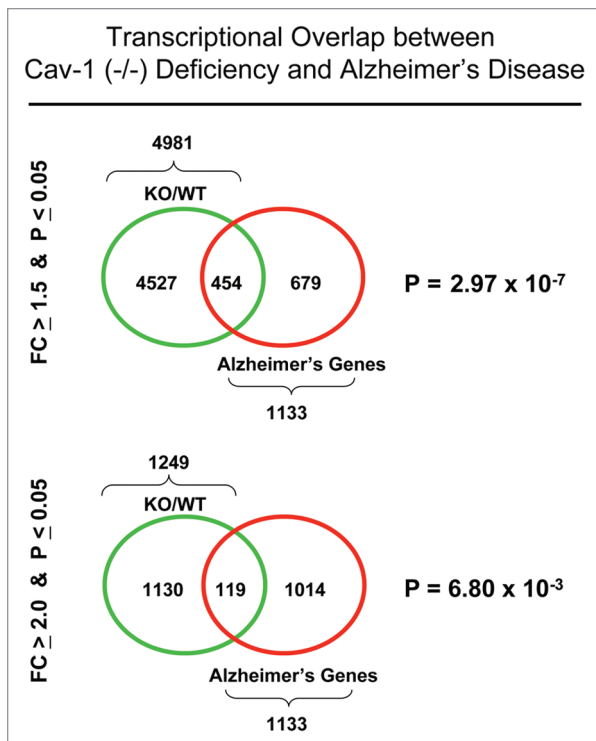


Figure 11. Venn diagrams for the transcriptional overlap between Cav-1 (-/-) stromal deficiency and Alzheimer disease. Upper, using a fold-change cut-off of 1.5 for Cav-1 deficient stromal cells (KO/WT) ($p \leq 0.05$). Note the overlap of 454 genes with a p -value of 3×10^{-7} . Lower, using a fold-change cut-off of 2.0 for Cav-1 deficient stromal cells (KO/WT) ($p \leq 0.05$). Note the overlap of 119 genes with a p -value of 6.8×10^{-3} .

were quenched with 50 mM NH₄Cl in PBS/CM for 10 minutes at room temperature. Fixed cells were incubated for 1 hour at room temperature with anti-nitrotyrosine IgG (cat# 06-284 rabbit polyclonal, 1:200, Millipore, Inc.) in IF buffer. Cells were washed extensively with IF buffer, then incubated with secondary antibodies (Jackson Laboratories) for 30 minutes at room temperature, stained with DAPI (Sigma) and mounted with Pro-Long gold anti-fade reagent (Molecular Probes).

Immuno-capture of mitochondrial complex I. For immuno-precipitation of Mitochondrial Complex I, whole cell lysates of either mouse bone marrow derived stromal cells (BMSCs) (Wildtype or Cav1 (-/-)) or siRNA-treated hTERT-BJ1 human fibroblasts (*Cav1* siRNA or Control siRNA) were used. Cells were lysed for 1 hour at 4°C in lysis buffer containing 50 mM Tris-HCl, pH 8.0, 150 mM NaI, 1% *n*-dodecyl-β-D-maltoside (cat # MS910; Mitosciences, Inc.), plus Roche Complete Mini protease inhibitor cocktail. Cleared cell lysates (350 µg for hTERT-BJ1 cells or 100 µg for BMSCs) were incubated with a 5-µl bead-volume of Complex I immuno-capture beads (cat # MS101; Mitosciences, Inc.) and the suspension was allowed to bind overnight at 4°C while rotating. Beads with bound Complex I were serially washed four times with lysis buffer, high salt wash buffer (50 mM Tris-HCl, pH 8.0, 500 mM NaCl, 0.5% *n*-dodecyl-β-D-maltoside), low salt wash buffer (50 mM Tris-HCl, pH 8.0, 0.05% *n*-dodecyl-β-D-maltoside), and

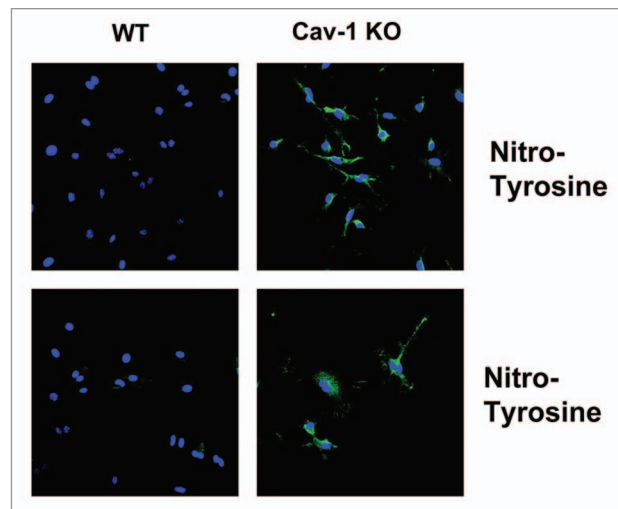


Figure 12. Cav-1 (-/-) deficient stromal cells show increased nitro-tyrosine staining. Cav-1 (-/-) deficient stromal cells (from bone marrow) were subjected to immuno-fluorescence analysis using a nitro-tyrosine specific antibody probe. Note that nitro-tyrosine staining (green) was more intense in Cav-1 (-/-) deficient stromal cells, as compared with WT stromal cells processed in parallel, as predicted.

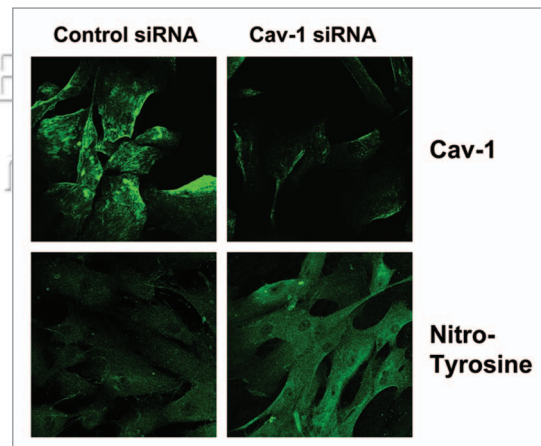


Figure 13. Acute knockdown of Cav-1 in fibroblasts increases nitro-tyrosine staining. We acutely downregulated Cav-1 expression in a human fibroblast cell line (hTERT-BJ1 cells), using an siRNA approach with oligonucleotides (Cav-1 siRNA versus an siRNA control). Note that this siRNA approach using transiently transfected human fibroblasts successfully knocked-down Cav-1 expression, resulting in the accumulation of nitro-tyrosine species. As such, loss of Cav-1 in stromal cells is associated with the over-production of NO and tyrosine nitration.

Pre-elution wash buffer (10 mM Tris-HCl, pH 6.8, 0.05% *n*-dodecyl-β-D-maltoside). The immuno-precipitated Complex I was eluted with 0.1 M glycine-Cl pH 1.5 and 1% SDS, and samples were neutralized with 1/8 volume of 1.5 M Tris-Cl, pH 8.8. Eluted samples were run on a 10% SDS-polyacrylamide gel (SDS-PAGE) under non-reducing conditions and transferred onto a nitrocellulose membrane, blocked in TBS-containing 5% BSA/0.05% Tween-20, and incubated with 1:1,000 dilution of an anti-nitro-tyrosine monoclonal antibody (mAb; cat # MS703;

Mito Complex I (IP) / Nitro-tyrosine (WB)

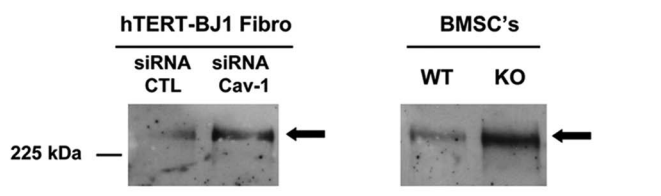


Figure 14. Loss of Cav-1 in stromal cells causes the accumulation of nitro-tyrosine in mitochondrial complex I. To determine if the respiratory chain might be one of the targets of tyrosine nitration, we immunoprecipitated mitochondrial complex I from whole cell lysates. These immunoprecipitates were then subjected to western blot analysis. Note that nitro-tyrosine selectively accumulated in a >225 kDa component of mitochondrial complex I, and tyrosine nitration was dramatically increased in the absence of Cav-1. Virtually identical results were obtained with both Cav-1 (-/-) deficient stromal cells (right) and fibroblasts transiently transfected with Cav-1 siRNA (left), processed in parallel. As such, loss of Cav-1 may result in the inactivation of mitochondrial complex I via tyrosine nitration.

Loss of Stromal Cav-1

Increased Nitric Oxide (NO)

Mitochondrial Dysfunction

ROS/Oxidative Stress/Myo-fibroblast

HIF ↔ NF-κB

Aerobic Glycolysis Inflammation

The Reverse Warburg Effect

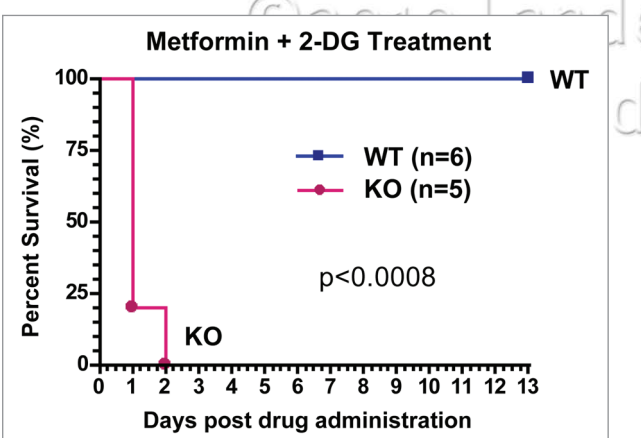


Figure 15. Metabolic restriction with chemical inhibitors is synthetically lethal with a Cav-1 (-/-) deficiency in mice. We reasoned that if Cav-1 (-/-) deficient mice suffer from mitochondrial dysfunction, then they will have a reduced mitochondrial reserve capacity. For this purpose, we used metformin (a mitochondrial complex I inhibitor) and 2-DG (2-deoxy-glucose; a glycolysis inhibitor). Briefly, WT and Cav-1 (-/-) deficient mice were starved for 4 hours, and injected (i.p.) with metformin (300 mg/kg/day) or 2-DG (500 mg/kg/day), either individually or in combination. Administration of metformin or 2-DG individually did not seriously affect the WT or Cav-1 (-/-) deficient mice, all of which quickly recovered (data not shown). However, the combination of metformin and 2-DG in Cav-1 (-/-) deficient mice was lethal. Eighty-percent of the Cav-1 (-/-) deficient mice injected died on day 1, and 100% died by day 2 ($p < 0.0008$). WT mice injected daily with the combination (Met + 2-DG) were followed for at least 13 days and showed no deaths.

Figure 16. A working hypothesis for how a loss of stromal fibroblast Cav-1 drives the “reverse Warburg effect”. Based on an informatics analysis, we propose that a loss of stromal Cav-1 leads to oxidative stress in fibroblasts, which can then activate key transcription factors, such as HIF and NF κ B, driving aerobic glycolysis, inflammation, and angiogenesis, in the tumor micro-environment. We also identified and validated a possible mechanism for promoting oxidative stress in Cav-1 (-/-) deficient stromal cells: mitochondrial dysfunction. Experimentally, we showed that Cav-1 (-/-) deficient stromal cells have (i) increased tyrosine nitration (indicative of the over-production of peroxynitrite), and that (ii) the tyrosine nitration of mitochondrial complex I occurs. Consistent with this notion, we demonstrated that Cav-1 (-/-) deficient mice have a dramatically reduced mitochondrial reserve capacity, when challenged with chemically-induced metabolic restriction with a mitochondrial complex I inhibitor (metformin) and a glycolysis inhibitor (2-deoxy-glucose). In this context, metabolic restriction was synthetically lethal with a Cav-1 deficiency. Thus, chemically-induced metabolic restriction may be a new therapeutic strategy to target Cav-1 deficient stromal cells that promote tumor growth and metastasis. It is important to note that ROS/oxidative stress is known to be sufficient to drive the myofibroblast differentiation program in fibroblasts,⁹⁶⁻⁹⁹ and ROS/oxidative stress is also known to be sufficient to activate HIF and NF κ B transcriptional programs.^{15,16,18} Similarly, it is also known that a loss of Cav-1 increases NO and/or ROS production,²⁰⁻²³ and it is known that NO over-production leads to mitochondrial dysfunction,²⁴⁻³² and that mitochondrial dysfunction further drives ROS production.¹⁰⁰ So, all the individual steps in this new pathway have already been clearly demonstrated experimentally.

Mitosciences, Inc.,) at 4°C overnight. Membranes were washed extensively in TBS containing 0.3% Tween-20, probed with a secondary anti-mouse IgG-HRP antibody, and visualized with an enhanced chemi-luminescent reagent (Pierce, Inc.).

Animals. All animals were housed and maintained in a pathogen-free environment/barrier facility at the Kimmel Cancer Center at Thomas Jefferson University according to the guidelines of the National Institutes of Health. Mice were kept on a 12-hour light/dark cycle with ad libitum access to chow and water. Cav-1 (-/-) deficient mice were generated, as we previously described. All mice used for drug treatments were in the C57BL/6 genetic background. Animal protocols used for this study were pre-approved by the institutional animal care and use committee.

Chemically-induced metabolic restriction. Adult C57BL/6 male mice, 4–5 months of age (wild-type and Cav-1 (-/-)) were injected intra-peritoneally with 2-deoxy-glucose (cat# D6134; 2DG) (500 mg/kg) (Sigma), and Metformin (300 mg/kg) (cat# D150959; Sigma) dissolved in sterile PBS. Injections were administered on a daily basis, at the same time each day, and after 4 hours of fasting. All remaining WT mice were sacrificed after 13 days, at the end of the experiment.

Conclusions

In summary, here we have used a proteomics-guided informatics analysis to identify the major signaling and transcriptional pathways that are activated in Cav-1 (-/-) deficient stromal cells. These results point towards oxidative stress, which mimics hypoxia, and drives inflammation. As such, it is these signaling and transcriptional programs in cancer-associated fibroblasts which would be expected to drive increased tumor growth, recurrence, metastasis, and poor clinical outcome in breast cancer patients lacking stromal Cav-1. Notably, DCIS patients lacking stromal Cav-1 showed a strong association with the presence of inflammatory cells in the DCIS local micro-environment, which was also associated with progression to invasive breast cancer.⁹

References

- Bissell MJ, Radisky D. Putting tumours in context. *Nat Rev Cancer* 2001; 1:46-54.
- Bissell MJ, Radisky DC, Rizki A, Weaver VM, Petersen OW. The organizing principle: microenvironmental influences in the normal and malignant breast. *Differentiation* 2002; 70:537-46.
- Ghajar CM, Meier R, Bissell MJ. Quis custodiet ipsos custodes: who watches the watchmen? *Am J Pathol* 2009; 174:1996-9.
- Ronnov-Jessen L, Bissell MJ. Breast cancer by proxy: can the microenvironment be both the cause and consequence? *Trends Mol Med* 2009; 15:5-13.
- Mercier I, Casimiro MC, Wang C, Rosenberg AL, Quong J, Allen KG, et al. Human Breast Cancer-Associated Fibroblasts (CAFs) Show Caveolin-1 Downregulation and RB Tumor Suppressor Functional Inactivation: Implications for the Response to Hormonal Therapy. *Cancer Biol Ther* 2008; 7:1212-25.
- Sotgia F, Del Galdo F, Casimiro MC, Bonuccelli G, Mercier I, Whitaker-Menezes D, et al. Caveolin-1^{-/-} null mammary stromal fibroblasts share characteristics with human breast cancer-associated fibroblasts. *Am J Pathol* 2009; 174:746-61.
- Witkiewicz AK, Dasgupta A, Sotgia F, Mercier I, Pestell RG, Sabel M, et al. An Absence of Stromal Caveolin-1 Expression Predicts Early Tumor Recurrence and Poor Clinical Outcome in Human Breast Cancers. *Am J Pathol* 2009; 174:2023-34.
- Witkiewicz AK, Casimiro MC, Dasgupta A, Mercier I, Wang C, Bonuccelli G, et al. Towards a new "stromal-based" classification system for human breast cancer prognosis and therapy. *Cell Cycle* 2009; 8:1654-8.
- Witkiewicz AK, Dasgupta A, Nguyen KH, Liu C, Kovarich AJ, Schwartz GF, et al. Stromal caveolin-1 levels predict early DCIS progression to invasive breast cancer. *Cancer Biol Ther* 2009; 8:1167-75.
- Di Vizio D, Morello M, Sotgia F, Pestell RG, Freeman MR, Lisanti MP. An Absence of Stromal Caveolin-1 is Associated with Advanced Prostate Cancer, Metastatic Disease and Epithelial Akt Activation. *Cell Cycle* 2009; 8:2420-4.
- Pavlides S, Whitaker-Menezes D, Castello-Cros R, Flomberg N, Witkiewicz AK, Frank PG, et al. The reverse Warburg effect: aerobic glycolysis in cancer associated fibroblasts and the tumor stroma. *Cell Cycle* 2009; 8:3984-4001.
- Williams TM, Sotgia F, Lee H, Hassan G, Di Vizio D, Bonuccelli G, et al. Stromal and Epithelial Caveolin-1 Both Confer a Protective Effect Against Mammary Hyperplasia and Tumorigenesis: Caveolin-1 Antagonizes Cyclin D1 Function in Mammary Epithelial Cells. *Am J Pathol* 2006; 169:1784-801.
- Nakamura Y, Yasuoka H, Tsujimoto M, Yoshidome K, Nakahara M, Nakao K, et al. Nitric oxide in breast cancer: induction of vascular endothelial growth factor-C and correlation with metastasis and poor prognosis. *Clin Cancer Res* 2006; 12:1201-7.
- Sloan EK, Ciocca D, Pouliot N, Natoli A, Restall C, Henderson M, et al. Stromal Cell Expression of Caveolin-1 Predicts Outcome in Breast Cancer. *Am J Pathol* 2009; 174:2035-43.
- Chandel NS. Mitochondrial regulation of oxygen sensing. *Adv Exp Med Biol* 2010; 661:339-54.
- Galkin A, Higgs A, Moncada S. Nitric oxide and hypoxia. *Essays Biochem* 2007; 43:29-42.
- Benita Y, Kikuchi H, Smith AD, Zhang MQ, Chung DC, Xavier RJ. An integrative genomics approach identifies Hypoxia Inducible Factor-1 (HIF-1)-target genes that form the core response to hypoxia. *Nucleic Acids Res* 2009; 37:4587-602.

Most importantly, these findings provide a systematic and rationale basis for future experimental studies aimed at functionally validating and dissecting the relevant molecular signaling pathways that contribute to the "reverse Warburg effect" in cancer-associated fibroblasts, and preventing poor clinical outcome in human breast and prostate cancer patients.

Acknowledgements

M.P.L. and his laboratory were supported by grants from the NIH/NCI (R01-CA-080250; R01-CA-098779; R01-CA-120876; R01-AR-055660), and the Susan G. Komen Breast Cancer Foundation. F.S. was supported by grants from the W.W. Smith Charitable Trust, the Breast Cancer Alliance (BCA), and a Research Scholar Grant from the American Cancer Society (ACS). P.G.F. was supported by a grant from the W.W. Smith Charitable Trust, and a Career Catalyst Award from the Susan G. Komen Breast Cancer Foundation. R.G.P. was supported by grants from the NIH/NCI (R01-CA-70896, R01-CA-75503, R01-CA-86072, and R01-CA-107382) and the Dr. Ralph and Marian C. Falk Medical Research Trust. The Kimmel Cancer Center was supported by the NIH/NCI Cancer Center Core grant P30-CA-56036 (to R.G.P.). Funds were also contributed by the Margaret Q. Landenberger Research Foundation (to M.P.L.).

This project is funded, in part, under a grant with the Pennsylvania Department of Health (to M.P.L.). The Department specifically disclaims responsibility for any analyses, interpretations or conclusions.

The authors would also like to thank Dr. Isidore Rigoutsos (IBM/Thomas Jefferson University) for his generous help and critical reading of the manuscript.

Note

Supplementary materials can be found at:
www.landesbioscience.com/supplement/PavlidesCC9-11-Sup.pdf

18. Yao H, Yang SR, Kode A, Rajendrasozhan S, Cai S, Adenuga D, et al. Redox regulation of lung inflammation: role of NADPH oxidase and NFkappaB signalling. *Biochem Soc Trans* 2007; 35:1151-5.
19. Lovas A, Radke D, Albrecht D, Yilmaz ZB, Moller U, Habenicht AJ, et al. Differential RelA- and RelB-dependent gene transcription in LTbetaR-stimulated mouse embryonic fibroblasts. *BMC Genomics* 2008; 9:606.
20. Razani B, Engelman JA, Wang XB, Schubert W, Zhang XL, Marks CB, et al. Caveolin-1 null mice are viable but show evidence of hyperproliferative and vascular abnormalities. *J Biol Chem* 2001; 276:38121-38.
21. Schubert W, Frank PG, Woodman SE, Hyogo H, Cohen DE, Chow CW, et al. Microvascular hyperpermeability in caveolin-1 (-/-) knock-out mice. Treatment with a specific nitric-oxide synthase inhibitor, L-name, restores normal microvascular permeability in Cav-1 null mice. *J Biol Chem* 2002; 277:40091-8.
22. Medina FA, de Almeida CJ, Dew E, Li J, Bonuccelli G, Williams TM, et al. Caveolin-1-deficient mice show defects in innate immunity and inflammatory immune response during *Salmonella enterica* serovar Typhimurium infection. *Infect Immun* 2006; 74:6665-74.
23. Zhao YY, Zhao YD, Mirza MK, Huang JH, Potula HH, Vogel SM, et al. Persistent eNOS activation secondary to caveolin-1 deficiency induces pulmonary hypertension in mice and humans through PKG nitration. *J Clin Invest* 2009; 119:2009-18.
24. Borutaite V, Brown GC. Rapid reduction of nitric oxide by mitochondria, and reversible inhibition of mitochondrial respiration by nitric oxide. *Biochem J* 1996; 315:295-9.
25. Borutaite V, Budriunaite A, Brown GC. Reversal of nitric oxide-, peroxynitrite- and S-nitrosothiol-induced inhibition of mitochondrial respiration or complex I activity by light and thiols. *Biochim Biophys Acta* 2000; 1459:405-12.
26. Borutaite V, Moncada S, Brown GC. Nitric oxide from inducible nitric oxide synthase sensitizes the inflamed aorta to hypoxic damage via respiratory inhibition. *Shock* 2005; 23:319-23.
27. Brown GC. Nitric oxide regulates mitochondrial respiration and cell functions by inhibiting cytochrome oxidase. *FEBS Lett* 1995; 369:136-9.
28. Brown GC. Nitric oxide inhibition of cytochrome oxidase and mitochondrial respiration: implications for inflammatory, neurodegenerative and ischaemic pathologies. *Mol Cell Biochem* 1997; 174:189-92.
29. Brown GC. Nitric oxide and mitochondrial respiration. *Biochim Biophys Acta* 1999; 1411:351-69.
30. Brown GC. Nitric oxide as a competitive inhibitor of oxygen consumption in the mitochondrial respiratory chain. *Acta Physiol Scand* 2000; 168:667-74.
31. Brown GC. Regulation of mitochondrial respiration by nitric oxide inhibition of cytochrome c oxidase. *Biochim Biophys Acta* 2001; 1504:46-57.
32. Brown GC. Nitric oxide and mitochondria. *Front Biosci* 2007; 12:1024-33.
33. Burkle A. DNA repair and PARP in aging. *Free Radic Res* 2006; 40:1295-302.
34. Burkle A, Beneke S, Muiras ML. Poly(ADP-ribosyl)ation and aging. *Exp Gerontol* 2004; 39:1599-601.
35. Burkle A, Diefenbach J, Brabeck C, Beneke S. Ageing and PARP. *Pharmacol Res* 2005; 52:93-9.
36. Martin-Oliva D, Aguilar-Quesada R, O'Valle F, Munoz-Gomez JA, Martinez-Romero R, Garcia Del Moral R, et al. Inhibition of poly(ADP-ribose) polymerase modulates tumor-related gene expression, including hypoxia-inducible factor-1 activation, during skin carcinogenesis. *Cancer Res* 2006; 66:5744-56.
37. Forner F, Kumar C, Luber CA, Fromme T, Klingenspor M, Mann M. Proteome differences between brown and white fat mitochondria reveal specialized metabolic functions. *Cell Metab* 2009; 10:324-35.
38. Samudio I, Fiegl M, Andreeff M. Mitochondrial uncoupling and the Warburg effect: molecular basis for the reprogramming of cancer cell metabolism. *Cancer Res* 2009; 69:2163-6.
39. Samudio I, Fiegl M, McQueen T, Clise-Dwyer K, Andreeff M. The warburg effect in leukemia-stroma cocultures is mediated by mitochondrial uncoupling associated with uncoupling protein 2 activation. *Cancer Res* 2008; 68:5198-205.
40. Razani B, Combs TP, Wang XB, Frank PG, Park DS, Russell RG, et al. Caveolin-1-deficient mice are lean, resistant to diet-induced obesity, and show hypertriglyceridemia with adipocyte abnormalities. *J Biol Chem* 2002; 277:8635-47.
41. Chen J, Capozza F, Wu A, Deangelis T, Sun H, Lisanti M, et al. Regulation of insulin receptor substrate-1 expression levels by caveolin-1. *J Cell Physiol* 2008; 217:281-9.
42. Petruschke T, Rohrig K, Hauner H. Transforming growth factor beta (TGFbeta) inhibits the differentiation of human adipocyte precursor cells in primary culture. *Int J Obes Relat Metab Disord* 1994; 18:532-6.
43. Garcia-Cardenas G, Martasek P, Silber-Masters BS, Skidd PM, Couet JC, Li S, et al. Dissecting the interaction between nitric oxide synthase (NOS) and caveolin: Functional Significance of the NOS caveolin binding domain in vivo. *J Biol Chem* 1997; 272:25437-40.
44. Cohen AW, Hnasko R, Schubert W, Lisanti MP. Role of caveolae and caveolins in health and disease. *Physiol Rev* 2004; 84:1341-79.
45. Schubert W, Sotgia F, Cohen AW, Capozza F, Bonuccelli G, Bruno C, et al. Caveolin-1(-/-) and caveolin-2(-/-)-deficient mice both display numerous skeletal muscle abnormalities, with tubular aggregate formation. *Am J Pathol* 2007; 170:316-33.
46. Cohen AW, Razani B, Schubert W, Williams TM, Wang XB, Iyengar P, et al. Role of caveolin-1 in the modulation of lipolysis and lipid droplet formation. *Diabetes* 2004; 53:1261-70.
47. Cohen AW, Schubert W, Brasamle DL, Scherer PE, Lisanti MP. Caveolin-1 expression is essential for proper nonshivering thermogenesis in brown adipose tissue. *Diabetes* 2005; 54:679-86.
48. Fernandez MA, Albor C, Ingelmo-Torres M, Nixon SJ, Ferguson C, Kurzchalia T, et al. Caveolin-1 is essential for liver regeneration. *Science* 2006; 313:1628-32.
49. Del Galdo F, Lisanti MP, Jimenez SA. Caveolin-1, transforming growth factor-beta receptor internalization, and the pathogenesis of systemic sclerosis. *Curr Opin Rheumatol* 2008; 20:713-9.
50. Del Galdo F, Sotgia F, de Almeida CJ, Jasmin JF, Musick M, Lisanti MP, et al. Decreased expression of caveolin-1 in patients with systemic sclerosis: Crucial role in the pathogenesis of tissue fibrosis. *Arthritis Rheum* 2008; 58:2854-65.
51. Jasmin JF, Mercier I, Dupuis J, Tanowitz HB, Lisanti MP. Short-term administration of a cell-permeable caveolin-1 peptide prevents the development of monocrotaline-induced pulmonary hypertension and right ventricular hypertrophy. *Circulation* 2006; 114:912-20.
52. Jasmin JF, Mercier I, Hnasko R, Cheung MW, Tanowitz HB, Dupuis J, et al. Lung remodeling and pulmonary hypertension after myocardial infarction: pathogenic role of reduced caveolin expression. *Cardiovasc Res* 2004; 63:747-55.
53. Svegliati S, Cancello R, Sambo P, Luchetti M, Paroncini P, Orlandini G, et al. Platelet-derived growth factor and reactive oxygen species (ROS) regulate Ras protein levels in primary human fibroblasts via ERK1/2. Amplification of ROS and Ras in systemic sclerosis fibroblasts. *J Biol Chem* 2005; 280:36474-82.
54. Sambo P, Baroni SS, Luchetti M, Paroncini P, Dusi S, Orlandini G, et al. Oxidative stress in scleroderma: maintenance of scleroderma fibroblast phenotype by the constitutive upregulation of reactive oxygen species generation through the NADPH oxidase complex pathway. *Arthritis Rheum* 2001; 44:2653-64.
55. De Felice B, Garbi C, Santoriello M, Santillo A, Wilson RR. Differential apoptosis markers in human keloids and hypertrophic scars fibroblasts. *Mol Cell Biochem* 2009; 327:191-201.
56. De Felice B, Wilson RR, Nacca M. Telomere shortening may be associated with human keloids. *BMC Med Genet* 2009; 10:110.
57. Felton VM, Borok Z, Willis BC. N-acetylcysteine inhibits alveolar epithelial-mesenchymal transition. *Am J Physiol Lung Cell Mol Physiol* 2009; 297:805-12.
58. Murthy S, Adamakova-Dodd A, Perry SS, Tephly LA, Keller RM, Metwali N, et al. Modulation of reactive oxygen species by Rac1 or catalase prevents asbestos-induced pulmonary fibrosis. *Am J Physiol Lung Cell Mol Physiol* 2009; 297:846-55.
59. Distler JH, Jungel A, Pileckyte M, Zwerina J, Michel BA, Gay RE, et al. Hypoxia-induced increase in the production of extracellular matrix proteins in systemic sclerosis. *Arthritis Rheum* 2007; 56:4203-15.
60. Hong KH, Yoo SA, Kang SS, Choi JJ, Kim WU, Cho CS. Hypoxia induces expression of connective tissue growth factor in scleroderma skin fibroblasts. *Clin Exp Immunol* 2006; 146:362-70.
61. Vincent AS, Phan TT, Mukhopadhyay A, Lim HY, Halliwell B, Wong KP. Human skin keloid fibroblasts display bioenergetics of cancer cells. *J Invest Dermatol* 2008; 128:702-9.
62. Zhang Q, Oh CK, Messadi DV, Duong HS, Kelly AP, Soo C, et al. Hypoxia-induced HIF-1alpha accumulation is augmented in a co-culture of keloid fibroblasts and human mast cells: involvement of ERK1/2 and PI-3K/Akt. *Exp Cell Res* 2006; 312:145-55.
63. Zhang Q, Wu Y, Ann DK, Messadi DV, Tuan TL, Kelly AP, et al. Mechanisms of hypoxic regulation of plasminogen activator inhibitor-1 gene expression in keloid fibroblasts. *J Invest Dermatol* 2003; 121:1005-12.
64. Zhang Q, Wu Y, Chau CH, Ann DK, Bertolami CN, Le AD. Crosstalk of hypoxia-mediated signaling pathways in upregulating plasminogen activator inhibitor-1 expression in keloid fibroblasts. *J Cell Physiol* 2004; 199:89-97.
65. Zhou G, Dada LA, Wu M, Kelly A, Trejo H, Zhou Q, et al. Hypoxia-induced alveolar epithelial-mesenchymal transition requires mitochondrial ROS and hypoxia-inducible factor 1. *Am J Physiol Lung Cell Mol Physiol* 2009; 297:1120-30.
66. Higgins DF, Biju MP, Akai Y, Wutz A, Johnson RS, Haase VH. Hypoxic induction of Ctgf is directly mediated by Hif-1. *Am J Physiol Renal Physiol* 2004; 287:1223-32.
67. Hickey MM, Richardson T, Wang T, Mosqueira M, Arguiri E, Yu H, et al. The von Hippel-Lindau Chuvala mutation promotes pulmonary hypertension and fibrosis in mice. *J Clin Invest* 2010; 120:827-39.
68. Kurylowicz A, Nauman J. The role of nuclear factor-kappaB in the development of autoimmune diseases: a link between genes and environment. *Acta Biochim Pol* 2008; 55:629-47.
69. Galindo M, Santiago B, Rivero M, Rullas J, Alcamí J, Pabllos JL. Chemokine expression by systemic sclerosis fibroblasts: abnormal regulation of monocyte chemoattractant protein 1 expression. *Arthritis Rheum* 2001; 44:1382-6.
70. Makino S, Mitsutake N, Nakashima M, Saenko VA, Ohtsuru A, Umezawa K, et al. DHMEQ, a novel NFkappaB inhibitor, suppresses growth and type I collagen accumulation in keloid fibroblasts. *J Dermatol Sci* 2008; 51:171-80.
71. Messadi DV, Doung HS, Zhang Q, Kelly AP, Tuan TL, Reichenberger E, et al. Activation of NFkappaB signal pathways in keloid fibroblasts. *Arch Dermatol Res* 2004; 296:125-33.
72. Zhu G, Cai J, Zhang J, Zhao Y, Xu B. Abnormal nuclear factor (NF)kappaB signal pathway and aspirin inhibits tumor necrosis factor alpha-induced NFkappaB activation in keloid fibroblasts. *Dermatol Surg* 2007; 33:697-708.

73. Di Giuseppe M, Gambelli F, Hoyle GW, Lungarella G, Studer SM, Richards T, et al. Systemic inhibition of NFκB activation protects from silicosis. *PLoS One* 2009; 4:e5689.
74. Henno P, Maurey C, Danel C, Bonnette P, Soulimas R, Stern M, et al. Pulmonary vascular dysfunction in end-stage cystic fibrosis: role of NFκB and endothelin-1. *Eur Respir J* 2009; 34:1329-37.
75. Wright JG, Christman JW. The role of nuclear factor kappa B in the pathogenesis of pulmonary diseases: implications for therapy. *Am J Respir Med* 2003; 2:211-9.
76. Rogai V, Lories RJ, Guiducci S, Luyten FP, Matucci Cerinic M. Animal models in systemic sclerosis. *Clin Exp Rheumatol* 2008; 26:941-6.
77. Pines M, Snyder D, Yarkoni S, Nagler A. Halofuginone to treat fibrosis in chronic graft-versus-host disease and scleroderma. *Biol Blood Marrow Transplant* 2003; 9:417-25.
78. Tyndall A, Furst DE. Adult stem cell treatment of scleroderma. *Curr Opin Rheumatol* 2007; 19:604-10.
79. Nash RA, McSweeney PA, Nelson JL, Wener M, Georges GE, Langston AA, et al. Allogeneic marrow transplantation in patients with severe systemic sclerosis: resolution of dermal fibrosis. *Arthritis Rheum* 2006; 54:1982-6.
80. Ueno NT, Rondon G, Mirza NQ, Geisler DK, Anderlini P, Giralt SA, et al. Allogeneic peripheral-blood progenitor-cell transplantation for poor-risk patients with metastatic breast cancer. *J Clin Oncol* 1998; 16:986-93.
81. Archer SL, Gomberg-Maitland M, Maitland ML, Rich S, Garcia JG, Weir EK. Mitochondrial metabolism, redox signaling and fusion: a mitochondria-ROS-HIF-1α-K_v1.5 O₂-sensing pathway at the intersection of pulmonary hypertension and cancer. *Am J Physiol Heart Circ Physiol* 2008; 294:570-8.
82. Bonnet S, Michelakis ED, Porter CJ, Andrade-Navarro MA, Thebaud B, Haromy A, et al. An abnormal mitochondrial-hypoxia inducible factor-1α-K_v1.5 channel pathway disrupts oxygen sensing and triggers pulmonary arterial hypertension in fawn hooded rats: similarities to human pulmonary arterial hypertension. *Circulation* 2006; 113:2630-41.
83. Rehman J, Archer SL. A proposed mitochondrial-metabolic mechanism for initiation and maintenance of pulmonary arterial hypertension in fawn-hooded rats: the warburg model of pulmonary arterial hypertension. *Adv Exp Med Biol* 661:171-85.
84. Zhao YY, Liu Y, Stan RV, Fan L, Gu Y, Dalton N, et al. Defects in caveolin-1 cause dilated cardiomyopathy and pulmonary hypertension in knockout mice. *Proc Natl Acad Sci USA* 2002; 99:11375-80.
85. Wunderlich C, Schmeisser A, Heerwagen C, Ebner B, Schobert K, Braun-Dullaeus RC, et al. Chronic NOS inhibition prevents adverse lung remodeling and pulmonary arterial hypertension in caveolin-1 knockout mice. *Pulm Pharmacol Ther* 2008; 21:507-15.
86. Bonuccelli G, Whitaker-Menezes D, Castello-Cros R, Pavlides S, Pestell RG, Fatas A, et al. The Reverse Warburg Effect: Glycolysis Inhibitors Prevent the Tumor Promoting Effects of Caveolin-1 Deficient Cancer Associated Fibroblasts. *Cell Cycle* 2010; 9:In Press.
87. Ozawa T, Okamura T, Harada T, Muraoka M, Ozawa N, Koyama K, et al. Accumulation of glucose in keloids with FDG-PET. *Ann Nucl Med* 2006; 20:41-4.
88. Chung SY, Lee JH, Kim TH, Kim SJ, Kim HJ, Ryu YH. ¹⁸F-FDG PET imaging of progressive massive fibrosis. *Ann Nucl Med* 2010; 24:21-7.
89. Klein M, Cohen-Cymberknoll M, Armoni S, Shoseyov D, Chisin R, Orevi M, et al. ¹⁸F-fluorodeoxyglucose-PET/CT imaging of lungs in patients with cystic fibrosis. *Chest* 2009; 136:1220-8.
90. Washino S, Hirai M, Matsuzaki A, Kobayashi Y. (18)F-Fluorodeoxyglucose positron emission tomography for diagnosis and monitoring of idiopathic retroperitoneal fibrosis associated with mediastinal fibrosis. *Ann Nucl Med* 2010; 24:225-9.
91. Shih GL, Shih WJ, Milan PP. FDG uptake in an abdominal surgical scar from an exploratory laparotomy. *Br J Radiol* 2009; 82:523-5.
92. Basu S, Baghel NS. Recurrence of dermatofibrosarcoma protuberans in post-surgical scar detected by ¹⁸F-FDG-PET imaging. *Hell J Nucl Med* 2009; 12:68.
93. Groves AM, Win T, Scretton NJ, Berovic M, Endozo R, Booth H, et al. Idiopathic pulmonary fibrosis and diffuse parenchymal lung disease: implications from initial experience with ¹⁸F-FDG PET/CT. *J Nucl Med* 2009; 50:538-45.
94. Nakajo M, Jinnouchi S, Tanabe H, Tateno R. ¹⁸F-fluorodeoxyglucose positron emission tomography features of idiopathic retroperitoneal fibrosis. *J Comput Assist Tomogr* 2007; 31:539-43.
95. Subramanian A, Tamayo P, Mootha VK, Mukherjee S, Ebert BL, Gillette MA, et al. Gene set enrichment analysis: a knowledge-based approach for interpreting genome-wide expression profiles. *Proc Natl Acad Sci USA* 2005; 102:15545-50.
96. Bondi CD, Manickam N, Lee DY, Block K, Gorin Y, Abboud HE, et al. NAD(P)H oxidase mediates TGFβ1-induced activation of kidney myofibroblasts. *J Am Soc Nephrol* 21:93-102.
97. Masamune A, Watanabe T, Kikuta K, Satoh K, Shimosegawa T. NADPH oxidase plays a crucial role in the activation of pancreatic stellate cells. *Am J Physiol Gastrointest Liver Physiol* 2008; 294:99-108.
98. Hecker L, Vitral R, Jones T, Jagirdar R, Luckhardt TR, Horowitz JC, et al. NADPH oxidase-4 mediates myofibroblast activation and fibrogenic responses to lung injury. *Nat Med* 2009; 15:1077-81.
99. Cucoranu I, Clempus R, Dikalova A, Phelan PJ, Ariyan S, Dikalov S, et al. NAD(P)H oxidase 4 mediates transforming growth factor-beta1-induced differentiation of cardiac fibroblasts into myofibroblasts. *Circ Res* 2005; 97:900-7.
100. Zimmerman MC, Zucker IH. Mitochondrial dysfunction and mitochondrial-produced reactive oxygen species: new targets for neurogenic hypertension? *Hypertension* 2009; 53:112-4.